An-Najah National University

Faculty of Graduate Studies

Modeling of Solar Energy Yield of a Fixed, Titled and Tracking Solar Collectors Under Clear sky Condition: A comparative Study

By

Ameera I. M. Bahati

Supervisor

Dr. Tamer Khatib

This Thesis is Submitted in Partial Fulfillment of the Requirements for the Degree of Master of Clean Energy and Conservation Strategy Engineering, Faculty of Graduate Studies, An-Najah National University, Nablus -Palestine.

2020

Modeling of Solar Energy Yield of a Fixed, Tilted, and Tracking Solar Collectors Under Clear Sky Condition: a Comparative Study

By

Ameera Bahati

This thesis was Defended Successfully on 28/07/2020 and Approved by:

Defense Committee Member	Signature
– Associate Prof.Dr Tamer Khatib / Supervisor	…………………………
– Dr. Samer Alsadi / External Examiner	…………………………
– Dr. Moien Omar / Internal Examiner	Dr. Moien Omar …………………………

Acknowledgement

To begin with, acclaim is to Allah for helping me in making this thesis possible.

I acknowledge, with deep gratitude and appreciation, the inspiration, encouragement, valuable time and continuous guidance given to me by my thesis supervisor associate professor Dr. Tamer Khatib.

I am also grateful to the members of the Thesis Committee for their time and effort in reviewing my work. Furthermore, I extend many thanks to my respected university, An-Najah National University, and its academic staff for helping me in completing my thesis by answering the inquires that I had during the preparation of this thesis.

To my family and to all of my friends, I really appreciate your kind support, your sweet words, and each moment we shared during the period of my study, you made my life easy and beautiful.

At long last, I might want to thank, everyone who was vital to the successful realization of the thesis, as well as expressing my apology that I could not mention personally one by one.

dedication

Oh, who proudly carry your name

Oh who I missed you since childhood

Oh my heart trembling to remind you

Oh, you who have entrusted me with God, I dedicate you my work "my father"

To the example of patience, optimism and hope

For everyone who is found after God and His Prophet, "my dear mother."

For my support, my strength, and my refuge after God

For those who prefer me over themselves

For those who show me what is the most beautiful in life, "my brothers and sisters."

To my eternal companion in my life, "Muhammad".

To all those with whom I have affection, relatives, and friends

To all of them

I dedicate this work

الإقرار

انا الموقع ادناه مقدم الرسالة التي تحمل عنوان

Modeling of solar energy yield of a fixed, titled and tracking solar collectors under clear sky condition: A comparative study

اقر ان ما اشتملت عليه هذه الرسالة انما هو نتاج جهدي الخاص باستثناء ما تمت الإشارة له حيثما ورد، وان هذه الرسالة ككل، او أي جزء منها لم يقدم من قبل لنيل اية درجة علمية او بحث علمي او بحثي لدى اية مؤسسة تعليمية او بحثية أخرى.

Declaration

The work provided in this thesis, unless otherwise referenced, is the researcher's own work, and has not been submitted elsewhere for any other degree or qualification.

Student Name: **اسم الطالب: اميرة إبراهيم مصطفى بهته**

Signature **التوقيع:**

Date **التاريخ:**

List of contents

List of figures

List of tables

List of Abbreviations

D_S	declination angle
N	day Number
EoT	Equation of time
B	Function of day no.
ST	actual solar time
LMT	local meridian time
LTM	Local time meridian
T_GMT	Greenwich Mean Time
(LOD)	Longitude angle.
$H_{sr,ss}$	angle of sunrise and sunset
L	latitude angle
HS	hour angle
STSR, STSS	sunrise and sunset solar time
TSR	actual solar time sunrise
TSS	actual solar time of sunset
A	altitude angle
ITOT	Total radiation in Horizontal surface
(IBH)	direct beam radiation in Horizontal surface
(IDH)	diffuse radiation in Horizontal surface
A	apparent extraterrestrial flux
K	dimensionless factor called optical depth
M	air mass ratio
C	Sky diffuse factor
IB	direct beam
IC_{TOT}	Total radiation in aligned surface
IDC	Diffuse radiation in aligned surface
IB_C	Beam radiation in aligned surface
IRC	reflected radiation in aligned surface
θ	zenith angle
ΦS	azimuth angle of the sun
ΦC	azimuth angle of the collector
β	tilt angle
PV	photovoltaic
ρ	albedo of the surface

i	incidence angle
IT_{TOT}	Total radiation in the tracking surface
IRT	reflection radiation on tracking surface
IBT	beam radiation on the tracking surface
ID_T	diffuse radiation on tracking surface
PLC	programmable logic controller
β1	Variable tilt angle
θt	Variable Zenith Angle

Modeling of solar energy yield of a fixed, titled and tracking solar collectors under clear sky condition: A comparative study

By

Ameera I. M. Bahati

Supervisor

Dr. Tamer Khatib

Abstract

The production of electric energy based on solar radiation is one of the most important priorities in the world of clean energy, and the biggest challenge has become to know which systems are the most productive of energy.

Through the current research, three models of PV systems classified according to their mechanism of work were dealt with, as follows:

The first type is the horizontal solar collector, the second is the tilted solar collector, and the last is the dual-axis tracking solar collector.

Using the Matlab program, and based on the clear sky conditions, it was expected the amount of solar radiation absorbed by each of the three systems, and the amount of electrical energy that can be produced in each of them during daylight hours throughout the summer season.

After that, it became clear that the solar collector system that contains the dual-axis tracker is the highest productivity of electrical energy, followed by the tilted system, and finally the horizontal one. Whereas, the quantity of electrical production of the three solar collector systems appeared as follows, from highest throughput to lowest, respectively

2366.75kWh , 2476.30kWh, 3709.71kWh. On the other hand, which is the economic side, the solar tracker proved to be the most economical, as despite its high price in its construction, it was the lowest price per kilowatt hour among the three systems, where the horizontal, inclined and tracker systems recorded the following prices respectively$0.206 ⁄kWh , 0.197$⁄kWh , and 0.183$⁄kWh.

While dual-axis solar tracking model is the only one among the models that study them, which consumes energy during its work because it contains a motor for movement in order to track the sun , this quantity consumed was very little as compared to produced energy , almost negligible. To find that this matter did not affect the survival of this model in the forefront in terms of productivity and economical.

Chapter one

Introduction

1.1 overview

Solar energy systems have appeared during the past two or three decades as one of the renewable energy sources that can be applied in the areas of energy production . It is now widely used in various industrial, domestic and commercial applications .Some of these systems contain a solar collector, designed to collect solar energy and convert it into electrical or thermal energy. In general, the amount of solar energy captured by the collector has become the primary factor for energy that is developed in various applications (Chia-Yen Lee, 2009).

The peak watt (Wp) is the most important factor for solar energy units, on which it depends on the classification of energy by a solar module illuminated under the standard conditions: 1000 w / m2 of solar energy density, 25 ° C of ambient temperature and an air mass of 1.5; That is, when the path through the atmosphere is 1.5 times that of when the sun is at noon). Depending on the effect of day / night variation and daily time in the presence of cloud-blocking sunlight, the average electrical energy produced by a solar cell over the year is about 20% of its Wp classification. Finally, we find that Wp is highly dependent on the radiation absorbed and dependent On the tilt angle (the angle between the collector and the ground line), several strategies have been developed that aim to improve the inclination angle and direction of the solar collectors designed for different geographic latitude or potential use periods (Mossadah and Kihani, 2009; Hj Mohd Yakup et al., 2001; Bari , 2000).

In the event that the photoelectric system tracks the sun, the energy output will increase to find that on days with high radiation and a large proportion of it was direct, relatively high radiation gains can be obtained depending on the tracking mechanism. Finally, we find that these gains can reach about 50% in clear days, and in winter, 300% compared to fixed-horizontal systems. as shown in Figure 1.1 (Society, 2005).

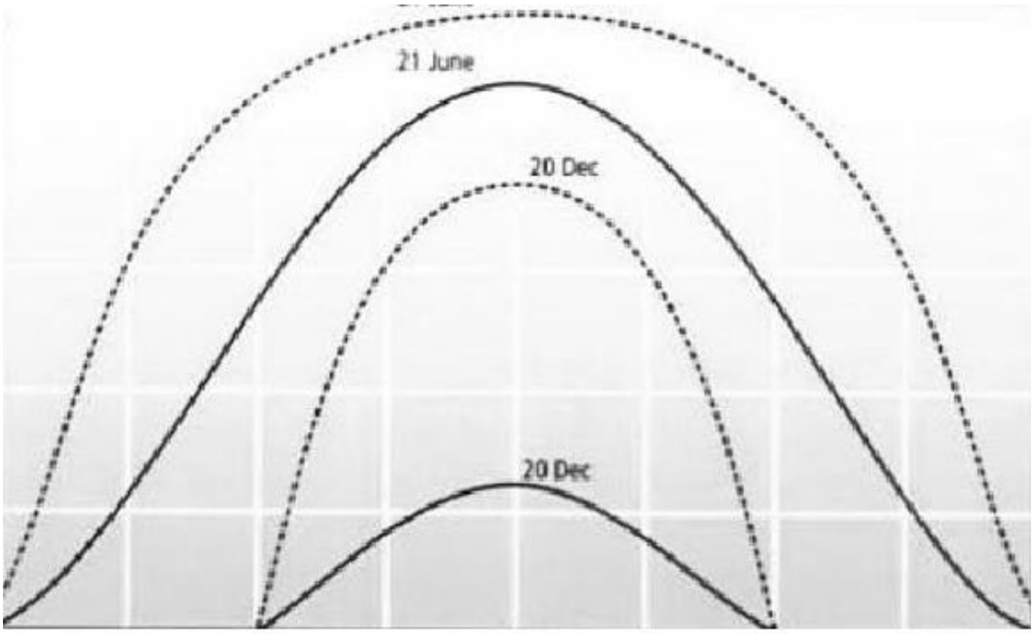

Figure 1.1*: Comparison of the tracking system with the non tracking systems*

1.2 Problem statement

In general active sun tracing systems have proven its accuracy as compared to fixed mounting systems. However, the feasibility of such systems is still questionable and thus, as assessment of energy consumption by these systems as compared to the energy gain should be conducted so as to judge its feasibility. In the meanwhile, iterative control algorithms might be more energy consuming and does not produce much more energy at the same time.

1.3 Research objectives

1- Modeling of Horizontal, tilted, and dual-Axis Sun Trackers for Photovoltaic Systems Using Matlab.

2- Calculating the electric energy produced and consumed from the systems under study.

3- Calculating the cost of energy from the systems under study.

3- Making a comparison between the three systems to find out the feasibility achieved from using the solar tracker.

1.4 Research methodology

WP.1 Literature review:

T. 1.1: Review research of the sun's geometry and the various models used to predict solar radiation of all kinds.

T. 1.2: Review a variety of research papers that mainly talk about photovoltaic systems. Especially those systems that contain the solar tracker of its various types to know the stage that this technique has reached.

WP.2: Data collection: Working on collecting information about the systems that work using the two-axis solar tracker to know the commercially available species and how much they consume and how much energy is

Produced. In addition, electrical specifications for these solar trackers.

WP.3 modeling of 2kWp PV system.

T. 3.1 modeling of horizontal algorithm.

T. 3.1 modeling of tilted surface algorithm

T. 3.3 modeling of dual –axes tracking algorithm.

WP.4 Assessment of viability of dual axis sun tracker for a mounting unit of 2-kWp PV system.

T. 4.1 calculating output energy produced by the PV array for summer season by each kind.

T. 4.2 calculation of energy consumption of the holding motor of tracking system.

WP.5 Thesis writing.

Chapter two

Literature review

2.1 overview

Scientists and researchers have given great importance to the renewable energy sector and the technology used in this field, so they have provided a lot of researches that will follow the development and permanent improvement of solar systems in general and focus on solar tracking systems.

After reviewing the previous researches, it became possible to revise the researches studied in this field based on several criteria as shown in the following charts.

Figure2.1 shows solar tracking system studies during the years, and we can note there is significant interest to the topic in the last five years. The application of tracking systems has been widely investigated.

***Figure 2.1** Solar tracking system studies during the years.*

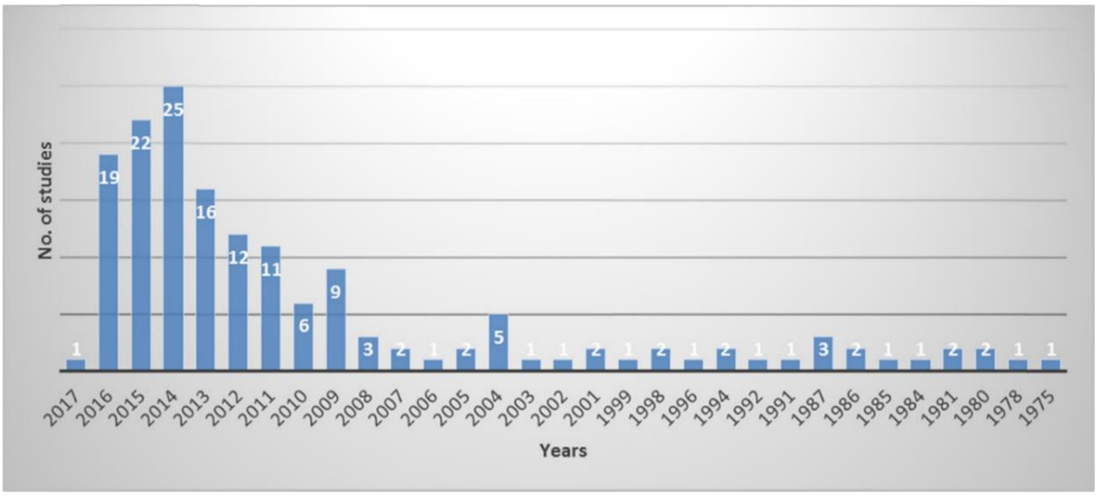

The studies in this field were divided into three axes based on the type of solar tracker regarding the direction of movement as shown in the following figure :

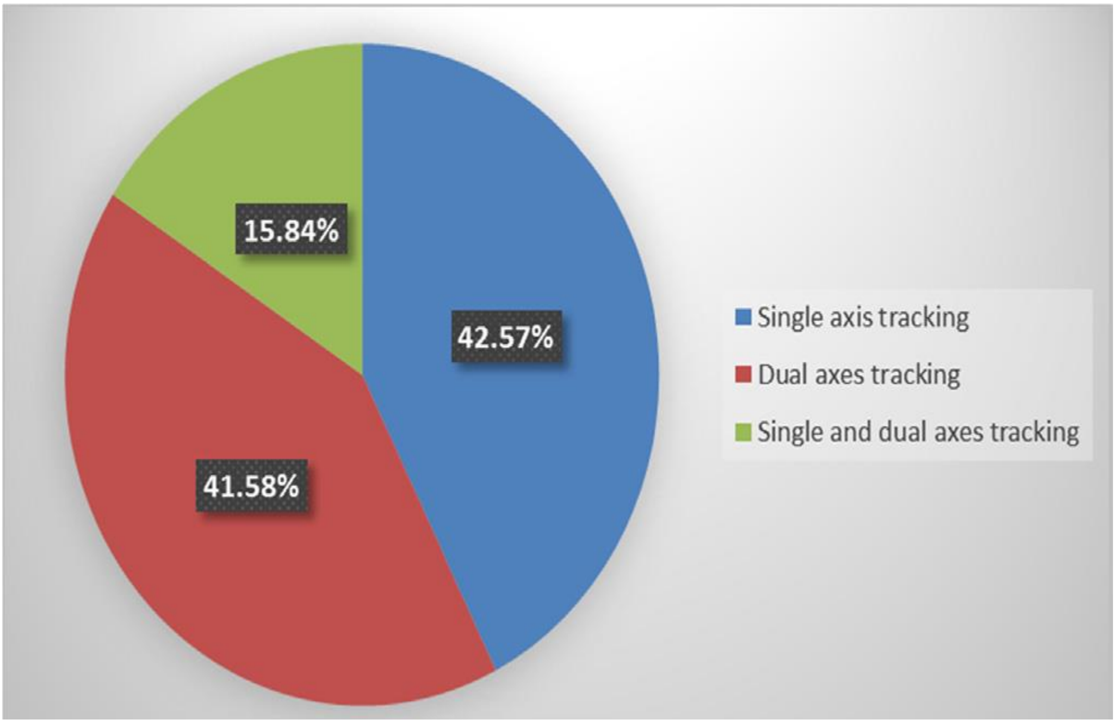

Figure 2.2 *Percentage of usage the solar tracking systems types in the studies.*

Moreover, the solar tracker drive systems are categorized into five types based on their tracking technologies, that is, active tracking, passive tracking, semi-passive tracking, manual tracking, and chronological tracking as shown the figure 2.3:

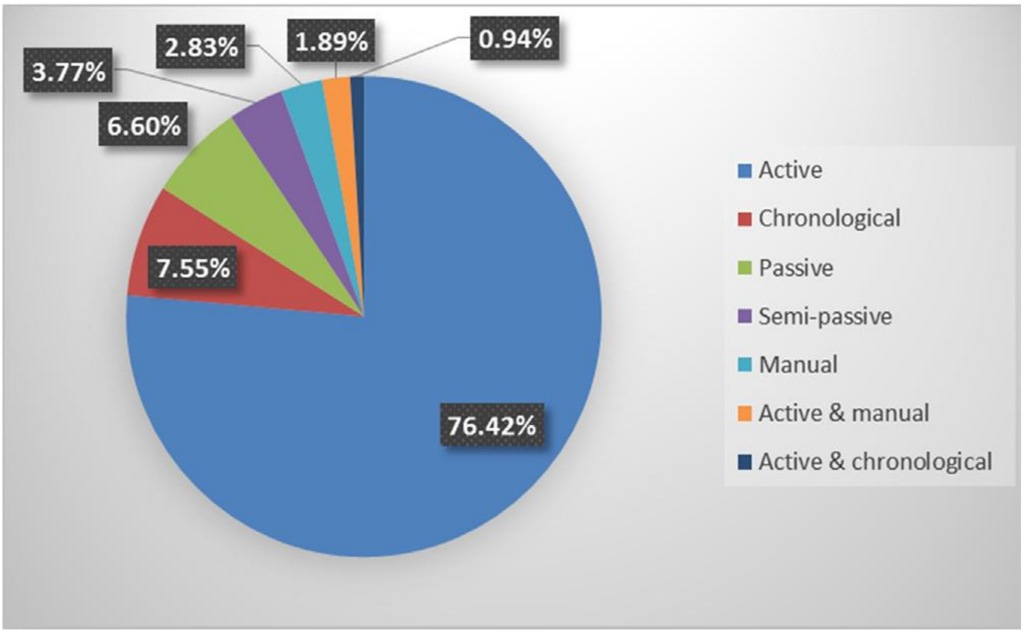

Figure 2.3: *Percentage of usage the solar tracking techniques in the recent studies.*

2.2 Dual axis solar tracking system

Fathabadi [1] suggested a sensor less dual-axis solar tracking system with a high accuracy controlled by the maximum powerpoint tracking unit of photovoltaic systems [1].

Hong et al. [2] presented a study of dual-axis tracker using direct and in-direct tracking methods aimed to generate greater electrical energy from smart photovoltaic panel. The following figure shows the types of tracking in the solar tracking systems in the dual-axis and single-axis. Meanwhile, the single axis works to track the path of the sun from east to west on a dai-ly basis, and this tracker can be classified into two types based on the axis of movement vertical and horizontal for a better performance in tracking solar energy. The other type, a dual-axis tracker that tracks the sun in both directions, combines the movement from east to west and north to south and can be classified into two types based on the axis of movement to find that the first type (tip-tilt dual axis tracker), which circulates around the horizontal axis and the slope of the panel's axis. In addition, the second type (azimuth-altitude dual axis tracker), which rotates around the vertical axis and the slope of panel axis [2].

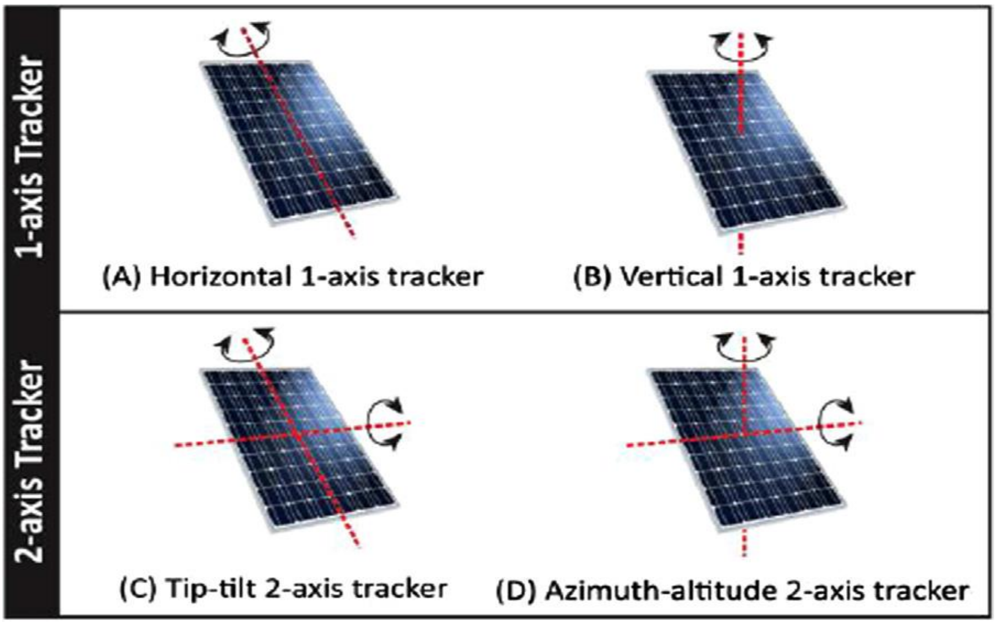

Figure 2.4: *Tracker types of Photovoltaic modules [2]*

Maya et al. [3] Developed a mathematical model that was applied to six different types of solar tracking systems in Brazil, with the aim of predicting absorbed energy, gaining useful energy ,and thermal efficiency of a flat solar collector, taking into account several factors, including the temperature of the water entering, the number of covers, and the emission from the flat. The six types of tracking used in evaluation are as following:

(R1) The collector rotated over a horizontal east–west axis with continued adjustment to lower the incidence angle.

(R2) The collector rotated over a horizontal north–south axis with continued adjustment to lower the incidence angle.

(R3) The collector with a constant slope rotated along a vertical axis. The tilt angle was taken equally to the absolute value of the local latitude.

(R4) The collector rotated over a north–south axis, parallel to the Earth's axis with continued adjustment to lower the incidence angle.

(R5) The collector with continued tracking along dual axes to lower the incidence angle.

(R6) a fixed collector slope oriented to north, with 20° tilt angle. [3].

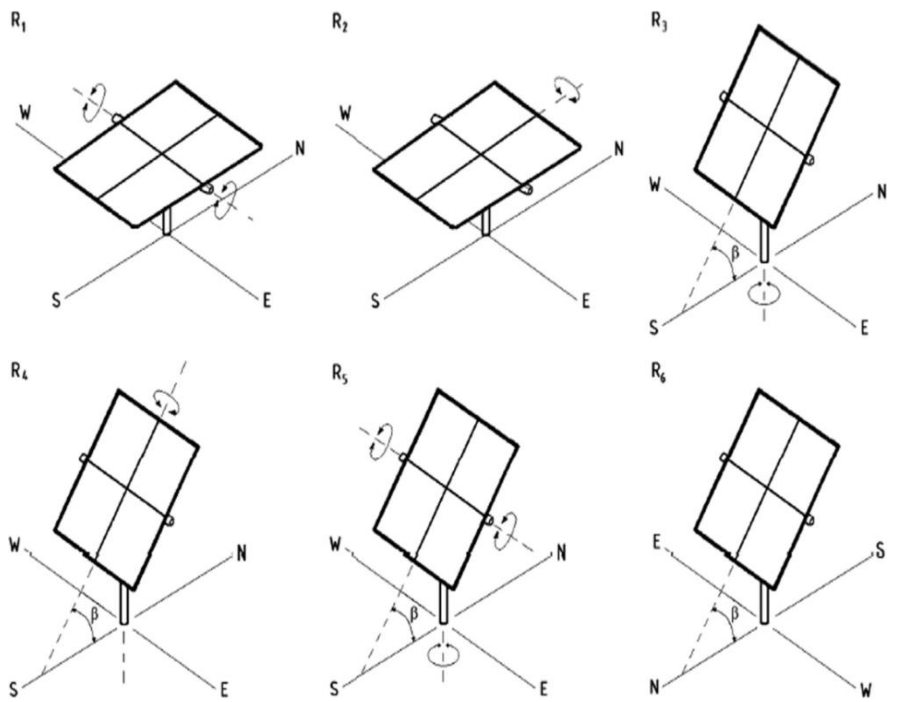

The figure2.5 show the six collector :

Figure2.5: *Tracking types of flat plate solar collectors [3]*

Gullen et al.[4] Developed Matlab code to validate experimental data from different types of collectors mode applied to solar multi-effect distillation plant. The purpose of this code was to calculate the amount of radiation received, the useful energy, heat loss from the parabolic collector and the production of fresh water for desalination of plants. In addition, the most appropriate tracking system for many altitudes has been proposed, taking into account the maximum standards for fresh water production. The following figure shows the types of tracking modes for parabolic trough collector used classified by means of motive mode:

(a) Full Tracking

(b) Polar axis tracking

(c) Single axis rotated over east-west (E-W tracking).

(d) Single axis rotated over north-south (N-S tracking).

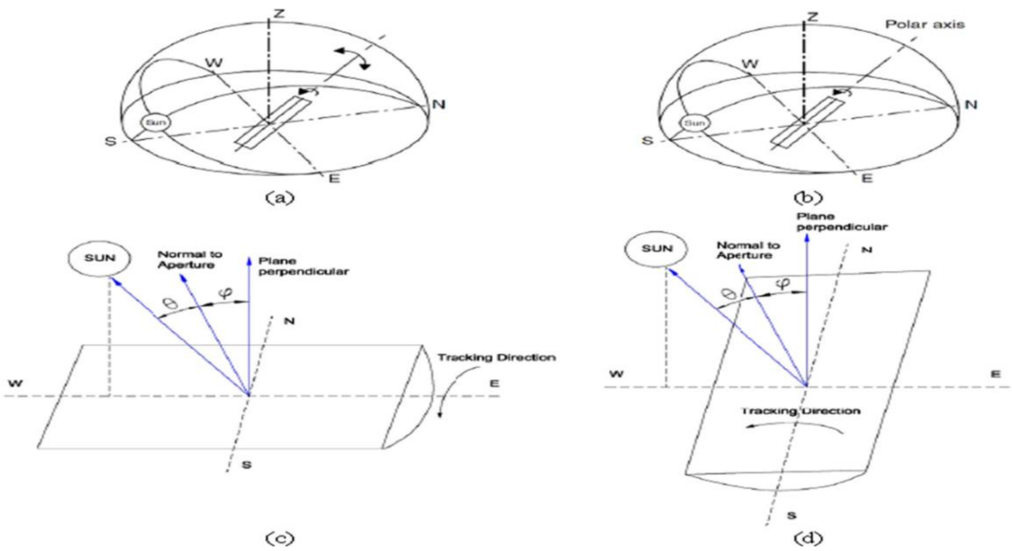

***Figure2.6**: Tracking modes for parabolic trough collector: (a) Full Tracking (b) Polar axis tracking (c) E-W tracking (d) N-S tracking [4]*

Sim and Stumberger [5] developed a new method of tracking the sun by photovoltaic systems that use a dual-axis tracker to find their optimal path. This method was applied to find optimal paths for the azimuth and tilt angle to obtain the maximum amount of energy produced. The success of this method was demonstrated by taking measurements using the stochastic search algorithm called differential evolution as an improvement tool, and comparing it with the expected values of solar radiation on photovoltaic panels. The energy consumed by the system was calculated during the steps of its implementation of the method to ensure its complete success. The following figure shows the dual axis sun tracking mechanical structure system. This system uses two motors (PMDC1, PMDC2) fed by 24-volt batteries to change the azimuth angle for east-west movement, and tilt angle for north-south movement respectively. The angles are changed by turning off and running the motors, which is controlled by a multi-stage gear [5]

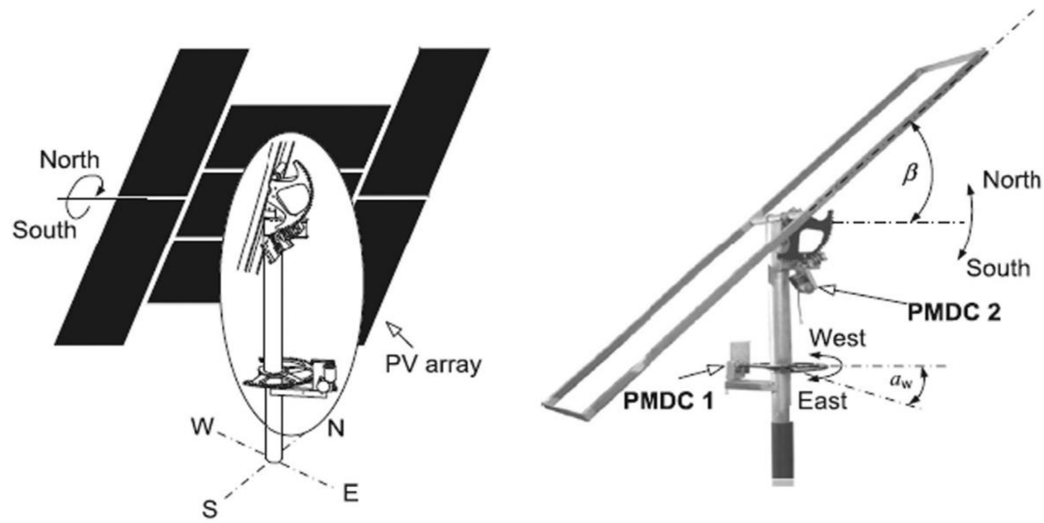

Figure2.7: *Dual-axis sun tracking system with changing azimuth angle αw and tilt angle β [5]*

Mei et al.[6] derive the equations of tracking for the target alignment heliostat in the solar tower power plants. Additionally, they designed a new unit with an asymmetric surface that was integrated through the HFLD code to analyze the target alignment heliostat. These derivative equations were validated for target-aligned heliostat with the toroidal surface and the image of the target alignment heliostat determined through the modified

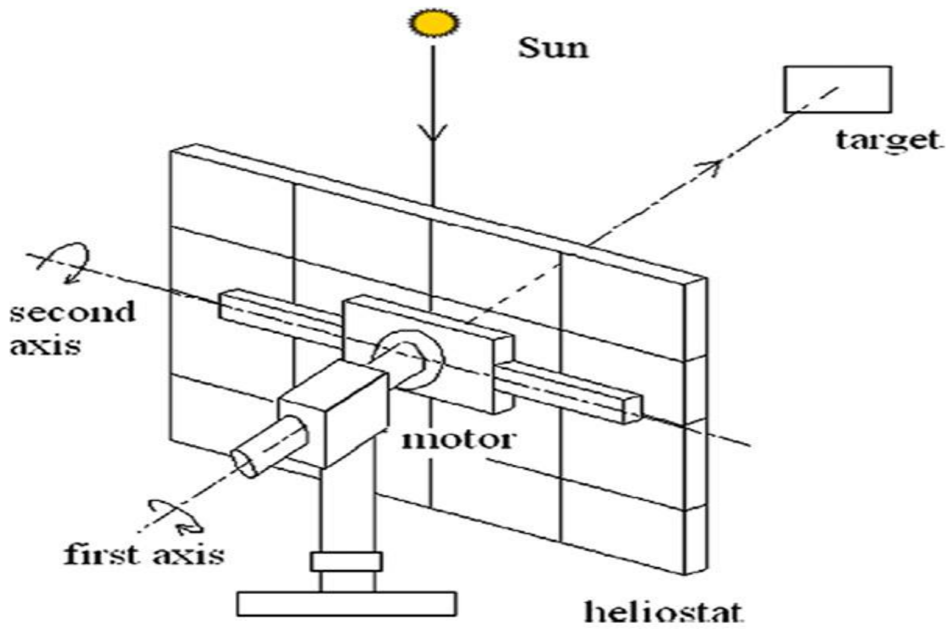

code HFLD by comparing it with the values calculated by the Zemax software.

Figure 2.8 *:The heliostat with target-aligned mount [6]*

The figure (2.8) shows the target alignment heliostat, which consists of two rotation axes the first, is geostationary and points toward the target and the second is perpendicular to the first axis and is located in the heliostat plane. Since the path of the sun changes during the day, so that the heliostat moves, and the movement done as following: First, the heliostat moves around the first axis until the incidence plane of the solar radiation in conjunction with the meridian plane of the heliostat, and then rotates around the second axis until it reflects the sun's rays towards the target.

Angles of Heliostat rotation can be calculated through:

1- Solar time.

2 - The location

3-The following figure shows the Cartesian right-handed coordinate systems of the deriving formulas of rotation angles of the target-aligned heliostat of the Heliostat on the ground.

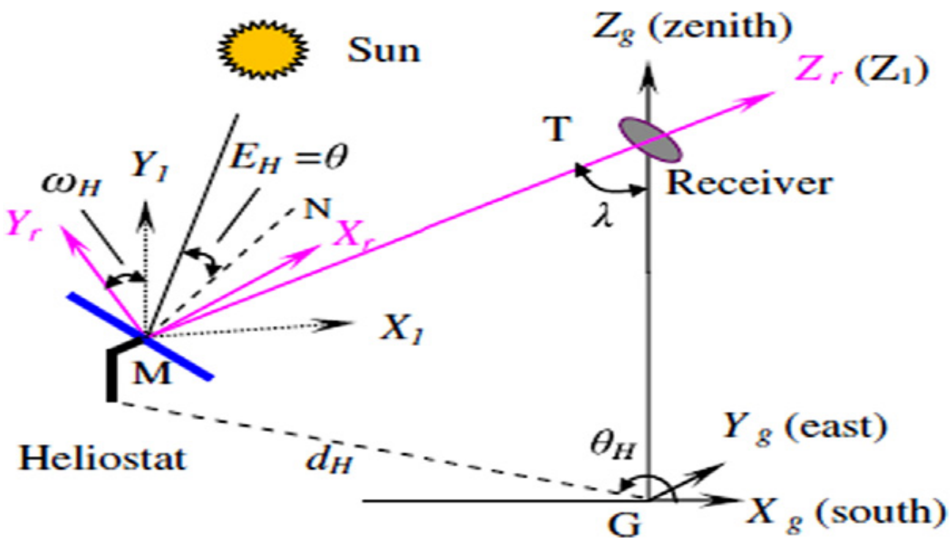

Figure 2.9*: Coordinate systems for deriving the rotation angle formulas for the target-aligned heliostat [6]*

The figures (10.a,10.b) show the incidence and reflection vectors that point to the sun from the target-aligned heliostat location in the ground co-ordinate, respectively .

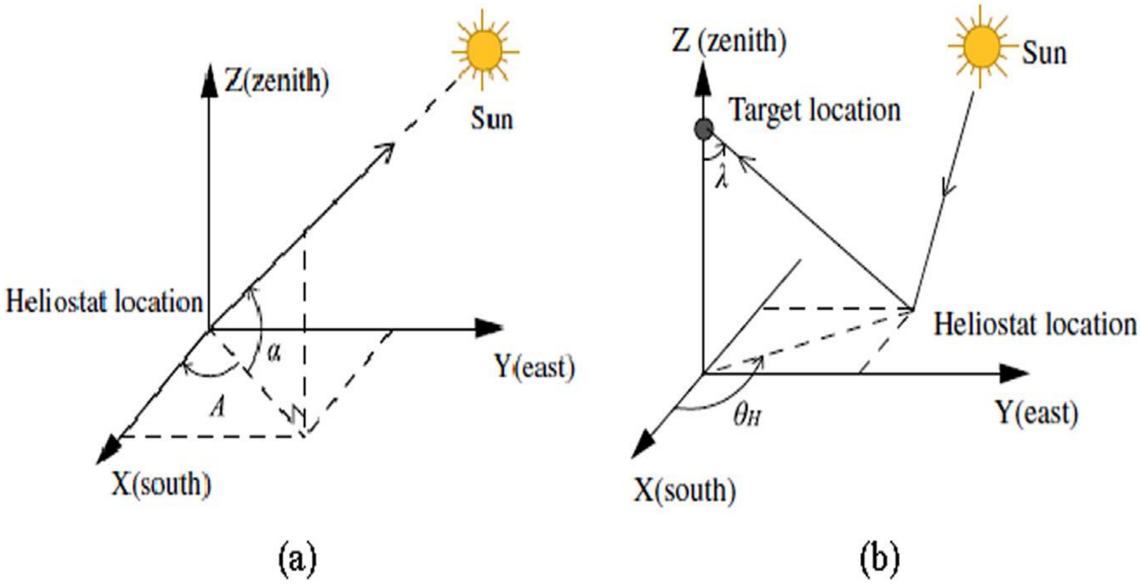

Figure2.10 (a) Incidence vector in ground-coordinates (b) Reflection vector in ground-coordinates [6]

The following figure consists of three cases of heliostat coordinates:

A - The coordinate system of the derived equations for the heliostat ray tracer shows the alignment of the target

B - Shows the transition coordinates from the heliostat coordinates to the normal reflection coordinates

C - Illustrates the coordinates of the transition from the coordinates of the reflection auxiliary to the coordinates of the target

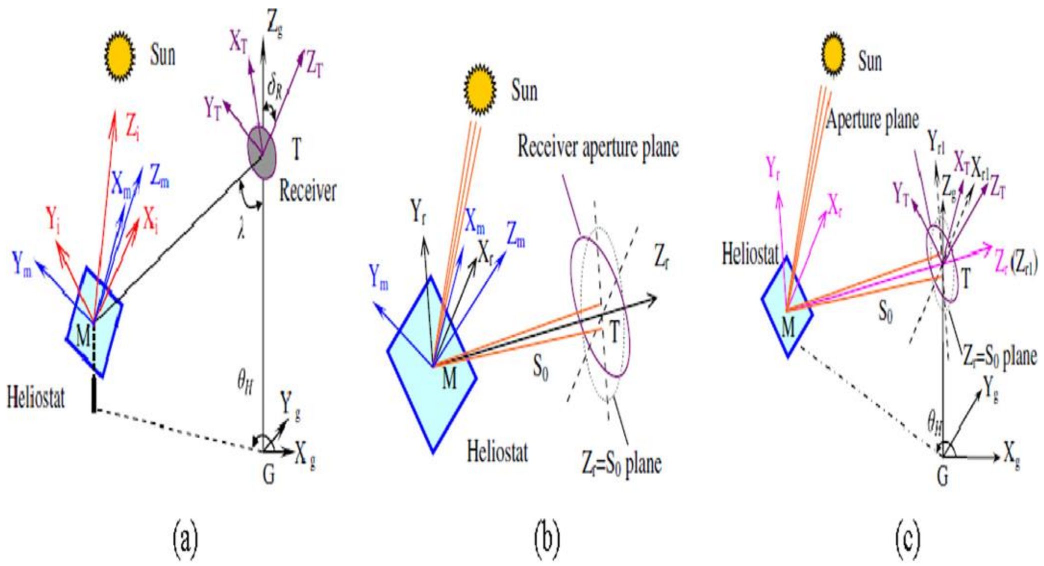

Figure2.11: *(a) Coordinate systems for deriving the ray tracing equations for the target-aligned heliostat (b) Coordinate transformation from heliostat coordinates to reflection-normal coordinates (c) Coordinate transformation from reflection auxiliary coordinates to target coordinates [6]*

2.3 Solar tracker drive types

In active tracking systems using microprocessors, and electro-optical sensors, the Sun is tracked using at least two PV cells or two LDRs. It then compares the output from the variable parameters, and then sends a signal, which is the difference between the two signals, to the drive. In solar tracking systems that contain bipolar auxiliary photovoltaic cells, these cells drive the drive system to the desired location. In solar tracking systems, which are driven by date and time, mathematical algorithms are calculated using the computer, and then a control signal is created for the system. This system is considered inaccurate in cloudy days because the sensors cannot make a decision because of the low solar irradiation, and therefore the intensity difference in the sensor signals is small [7].

Zogbi and Laplaze [8] they created a dual axis tracking system that tracks the movement of the Sun based on the azimuth and elevation angles. It is designed quadruple using two rectangular plans, and four sensors are installed in four sides. The signal from each pair of sensors is send then compared using a control circuit in the tracker containing an amplifier and several electronic components. This signal is sent to the motors to take the appropriate movement where the motor compares the signal coming from the magnifier and the value of the fixed threshold. In case the signal is larger than the fixed one, a decision shall be taken .At night, the system stops working and returns to the starting location [8].

Romla [9] Romla introduced a closed-loop solar tracking system based on the shadows method in 1996. Four photoresist sensors installed on a rigid platform containing two articulated arms supported by a camshaft engine was used. He placed the photoresist sensors under a pair of cylinders that were working to return the tracker from west to east and north to south. This tracker uses a control circuit consisting of a low-pass filter that represents the signal conditioning circuit and is then sent to the amplifier and then the signal is directed to the servomotor, to track and adapt the system based on the difference in sensing the solar radiation. The system stays at night in the same place turned off until a reboot works in the morning [9].

Das et al. [10] Introduced a design of a smart two-axis solar tracker using ATMEGA -8 L microcontroller plus four sensors installed on the tracker as shown in the figure[12.a]. Figure [12.b] shows the angle of incidence, which is the angle between sunlight and perpendicular to solar panels.

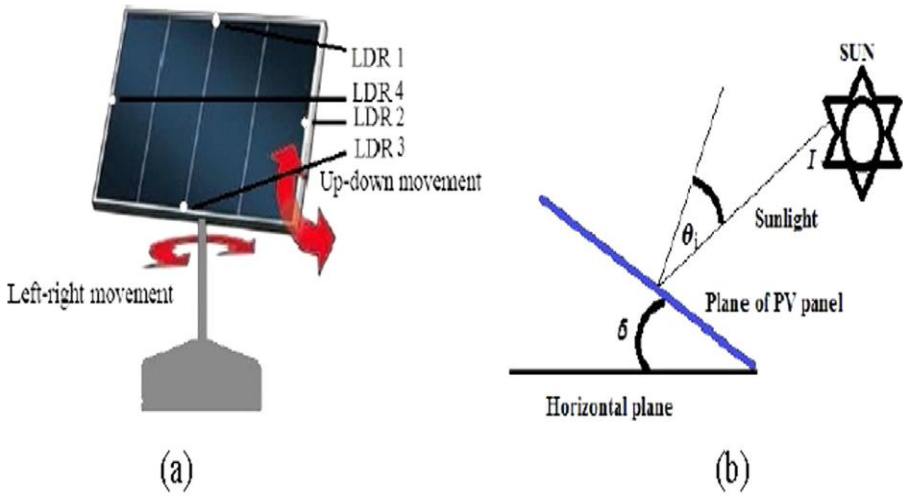

Figure2.12: *(a) Schematic diagram of smart dual-axis tracker (b) Angle of sunlight to the plane of photovoltaic panel [10]*

The following figure shows the front and back sides of a practical system of six solar panels connected in a series way, was mounted on a two-axis solar tracker located at the National Solar Energy Institute, India [10].

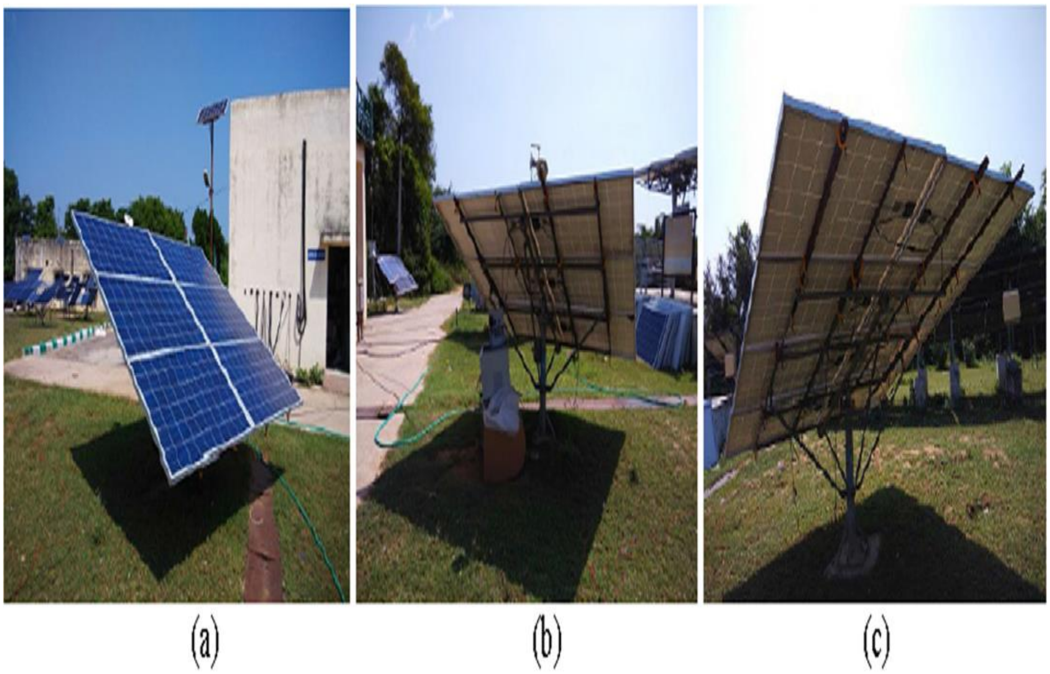

Figure2.13: *Experimental setup with (a) Front side of smart tracking system (b) Backside of smart tracking system (c) Backside of fixed photovoltaic panel system [10]*

Bentaher et al. [11] built and tested a simple tracking system based on two light dependent resistors. The optimal angle between the two resistances were calculated numerically and empirically. Determining the angle between the two light dependent resistors was considered as the accuracy of the system. The tracker contains an electric circuit based on LDR comparison through two amplifiers with a unity gain, as shown in the following figure.

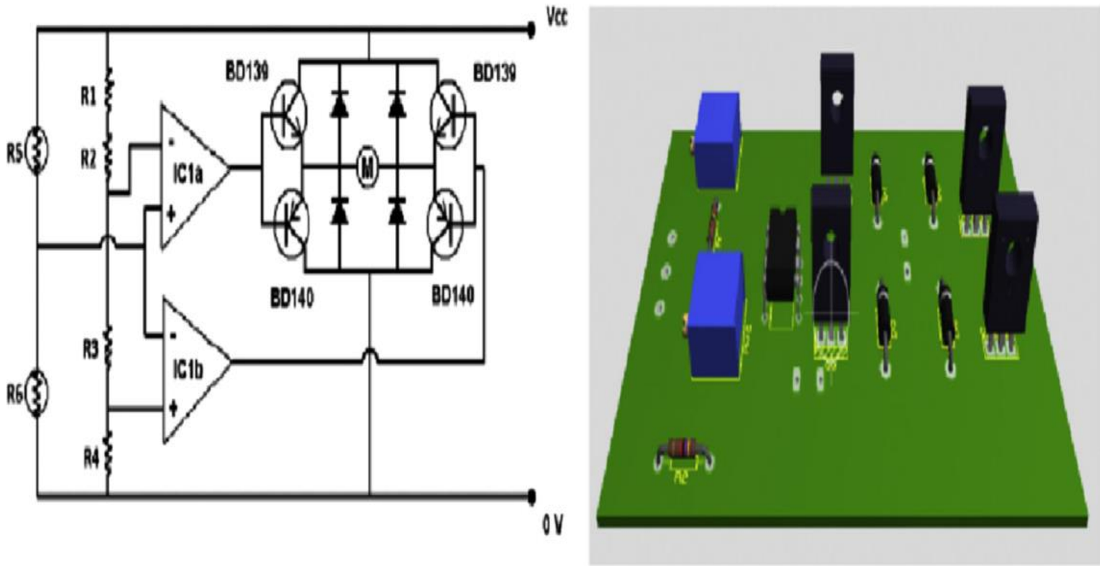

Figure2.14: *Electrical circuit, the two amplifiers IC1a and IC1b are in an integrated circuit LM1458 (National Semiconductor) [11]*

In order to verify that the difference in light dependent resistors depends on their orientation towards the sun, so that the light mechanism is adopted with an equivalent capacitor in the dual axis tracker. In addition, the tracker contains two DC motors to move the axis, and to control the movement two angular sensors were used, as shown in the figure (2.15).

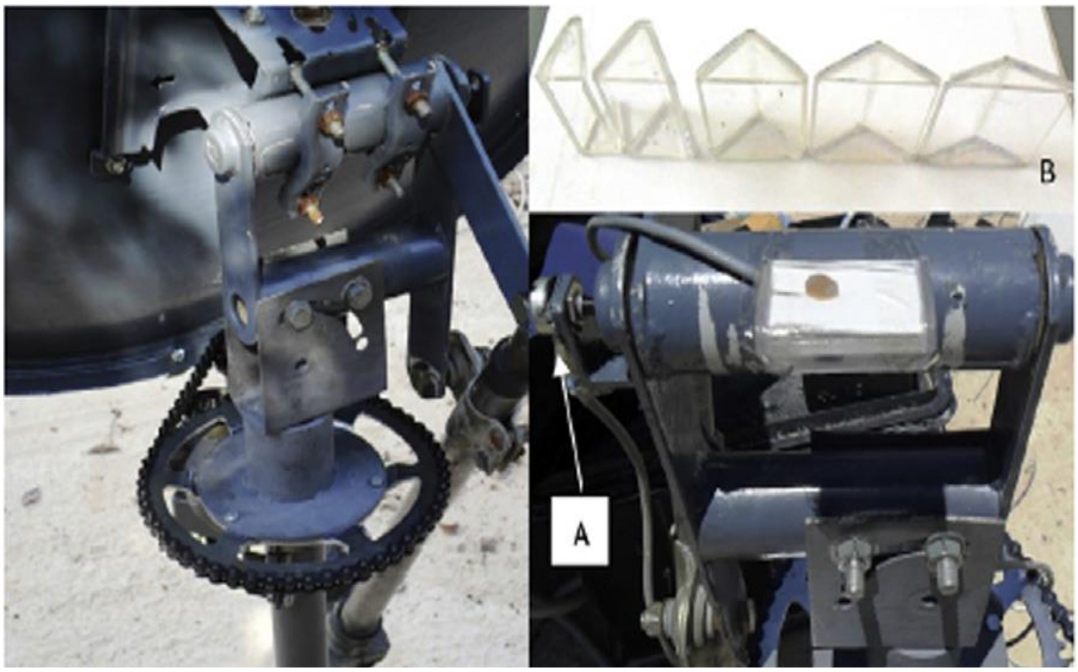

Figure 2.15: Experimental system (A) angular sensor, (B) pyramidal supports of sensors [11]

To track the change of direction of the sensor movement during the tracking the sun, angular rotation was used, and articulation axis keeping horizontally.

A pyramid sensor is used which illustrates the geometric form of the sensors where the effect of the beta angle is achieved in the accuracy of various pyramidal sensors (30 °, 60 °, 90 °, 120 ° and 140°). Light dependent resistor is measured at each position due to angular movement using digital multi-meters [11].

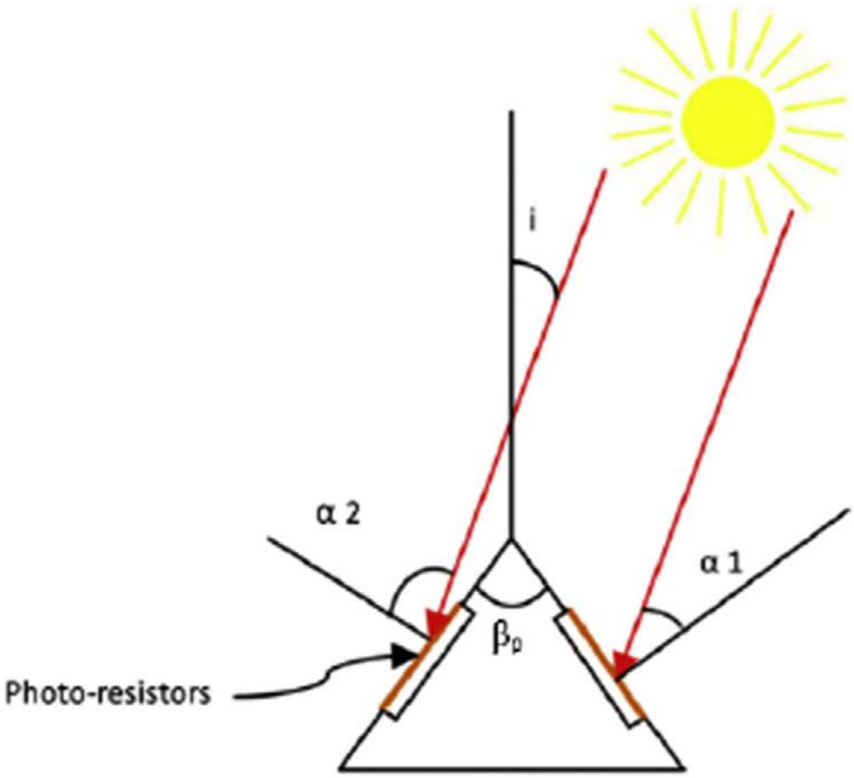

Figure 2.16: *Sensor geometry along with incidence angles [11]*

Parmar et al. [12] introduced a passive tracker that uses the heat of the sun to heat up water to move it by gravity this system is free of motors, gears and control circuits. The first system was designed in this way in 1969 The diagram below shows a 12pv system installed with a negative tracker, which delivered the same electric power as 15 photovoltaic modules. When compared between the two systems, it was found that the system using the passive solar tracker increased production by about 25% of that fixed system.

Figure2.17: *Universal Zomework model [12]*

In addition, the figure (2.17) shows a complete design of the passive solar tracker system with two canisters that are mounted on the edges of the frame, which the photovoltaic panels mounted on it, and the canisters keep connected through a metal tube. When the system is fully fixed on a vertical column, this means that the shadow will be fixed on the outer part of the metal canisters. As a result, the panels will be able to rotate to track the sun so that liquids moving inside the canisters will travel based on the high pressure of the liquid.

The figure (2.18) shows the four work mechanism

(A) At the beginning of the day, the sun rises from the east, and the direction of the system is to the west. The sun begins to heat up the unshaded western part of the canisters ,so that, the liquid moves towards the eastern part of the canisters through a tube made of a cooper rotating eastward.

(b) The process of heating the liquid is controlled through the shade of aluminum plates, when one of canisters face the sun longer than the other , Which leads to increase the pressure of steam, and force the liquid to cool from the shaded side. It causes a change in the weight of the liquid until the rack is forced to rotate and the shadows on the canisters are equal.

(c) The position of the sun changes during the day, so the rack marches by 15 degrees per hour until it reaches equilibrium because of fluid movement from one side to another.

(d) The rack continues moving westward during the rest of the day and remains in place during the night until the next morning.

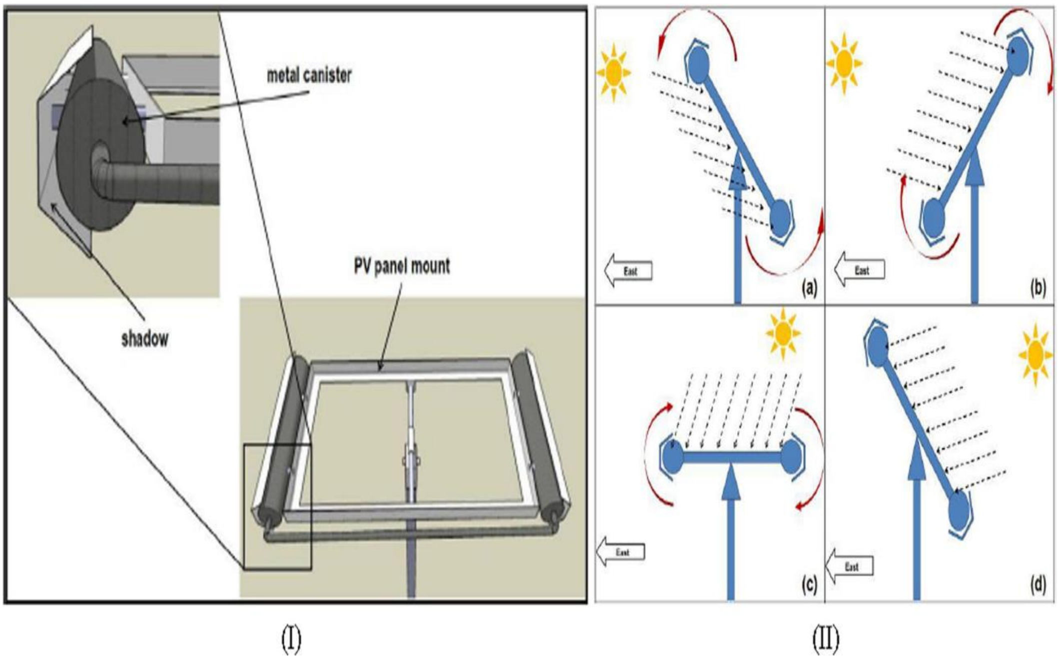

Figure2.18: *(I) Design of Solar Tracker; (II) Working Mechanism of Passive solar tracker [12]*

The passive solar tracking system consists of the following components:

1- Movable shade tapes with respect to canisters that change during summer and winter in order to control the temperature of the liquid inside the canisters.

2- Canisters and cylinders made of non-corrosive metal and coated in black color to ensure good cushioning of heat and these two packages are connected through a tube and when the temperature changes a pressure difference is produced to fill the canisters with liquid.

3- It uses balls to keep separation between the load bearing contexts in order to provide support for the load and to reduce the friction caused by rotation.

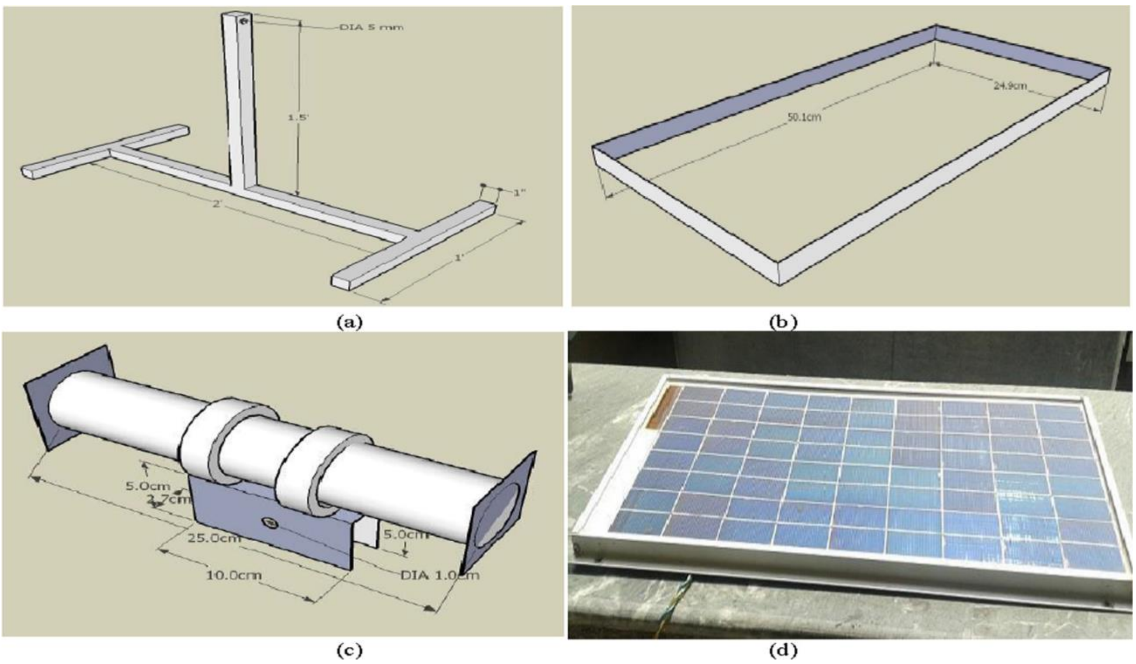

Figrue2.19*: Components of the solar tracker: (a) Base, (b) Frame, (c) Shafting and Bearings, (d) Solar Panel [12]*

Chapter three

Modeling of PV production considering horizontal, tilted and tracking PV panels

3.1 overview:

The mechanism of work in this research is structured to predict solar radiation from various types of solar panels during daylight hours throughout the summer season.

The types of solar panel placement focused on during the study are:

1- Horizontal.

2- Tilted angle.

3- Dual axis solar tracker.

In order to reach the required goal, it is necessary to work on defining the algorithms that govern the method of operation of these various systems mentioned above

Initially, there is a common and important step, which is to determine the hours of work based on a set of mathematical equations Depend's on the input information represented by today's number and geographic information about the place and other. These are detailed in the following sections

Then we will go through the process of predicting the amount of solar radiation absorbed for each type of systems adopted during each working hour throughout the year depending on the clear sky model

As a last step, we tend to work at the expense of the energy produced in each system, depending on the expected amount of solar radiation.

3.2 Modeling of sun position:

As a result of the continuous movement of the sun around the Earth, its location coordinates remain constantly changing throughout the day. It is crucial to determine the position of the sun while it is moving in the sky to control the position of the PV panels to remain perpendicular to the sun's rays as long as possible. In addition to that, work to determine daylight hours, which is the period of operation of solar systems.

The process of determining the coordinates of the position of the sun is carried out by a series of mathematical equations, started from the declination angle, which is the angle between the Earth–Sun vector and the equatorial plane, and this, is can be found by using following equation:

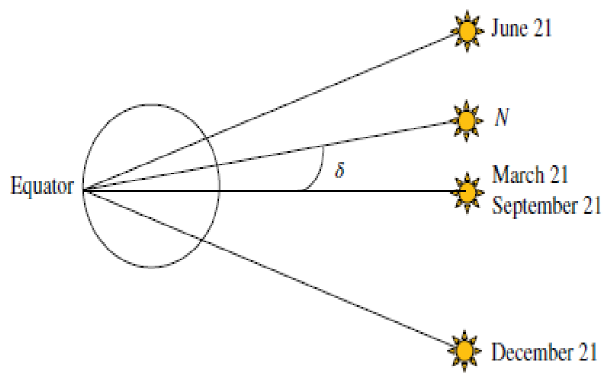

Figure 3.1*: solar declination angle*

$$D_S = 23.45° \left[\frac{(\text{sind}(360(N-81))}{365}\right] \tag{3.1}$$

In addition, Equation of time is a measure of the variation in the length of each day through the course of the year. Given by

$$\text{EoT} = 9.87\,\text{sind}(2B) - 7.53\,\text{cosd}\,B - 1.5\sin B \tag{3.2}$$

Where B can be calculated by

$$B = \frac{360}{364}\,(N - 81) \tag{3.3}$$

Where N is the day Number

Moreover, actual solar time (ST) is based on the apparent motion of the actual Sun. It is based on the apparent solar day, the interval between two successive returns of the Sun to the local meridian, which can be found by

$$\text{ST} = \text{LMT} + T_S\_\text{correction} \tag{3.4}$$

Where Ts_correction calculated by

$$T_S\_\text{correction} = \text{EoT} \pm 4\text{m}/°(\text{LTM} - \text{LOD}) \tag{3.5}$$

Where Local time meridian (LTM) equal to

$$\text{LTM} = 15°(\text{T\_GMT}) \tag{3.6}$$

(LOD) is longitude angle.

The current step is to determine the angle of sunrise and sunset to determine the duration of the day, so we turned to use the following equation:

$$H_{sr,ss} = \cos^{-1}(-\tan L \tan D_s) \tag{3.7}$$

Where L is latitude angle

After that, the hour angle that means the angle between the celestial meridian of an observer and the hour circle of a celestial object measured westward from the meridian can be calculated by:

$$HS = \frac{15°\left((ST-(12\times 60))\right)}{60} \tag{3.8}$$

This equation (3.8) used in calculated the sunrise and sunset solar time. The formula of this shown below:

$$STSR, STSS = (\frac{H_{sr,ss}}{15°} \pm 12) \times 60 \tag{3.9}$$

The actual solar time of sunset and sunrise time can be catch by the following equation:

$$TSR = STSR + |T_S\_correction| \tag{3.10}$$

$$TSS = STSS + |T_S\_correction| \tag{3.11}$$

The position of the sun during each hour is expressed by two main angles, which are the altitude angle (α) and the azimuth angle (ΦS).

Finding them is done by making use of what was found by the previous equations.

The altitude angle is the angle between the sun's rays and a horizontal plane, as shown in Figure (3.2). It is related to the solar zenith angle, θ, which is the angle between the sun's rays and the vertical. The altitude angle calculated by:

$$\sin\alpha = \sin L \sin D_S + \cos L \cos D_S \cos HS \qquad (3.12)$$

Where L is latitude angle , D_S is declination angle, HS is hour angle .Then,

$$\alpha = \text{sind}^{-1}(\sin\alpha) \qquad (3.13)$$

Azimuth angle is the angle of the sun's rays measured in the horizontal plane from due south for the Northern Hemisphere or due north for the Southern Hemisphere; westward is designated as positive. The mathematical expression for the solar azimuth angle is:

$$\sin(\Phi_S) = \frac{\text{sind}(HS)\ \text{cosd}(D_S)}{\text{cosd}\,\alpha} \qquad (3.14)$$

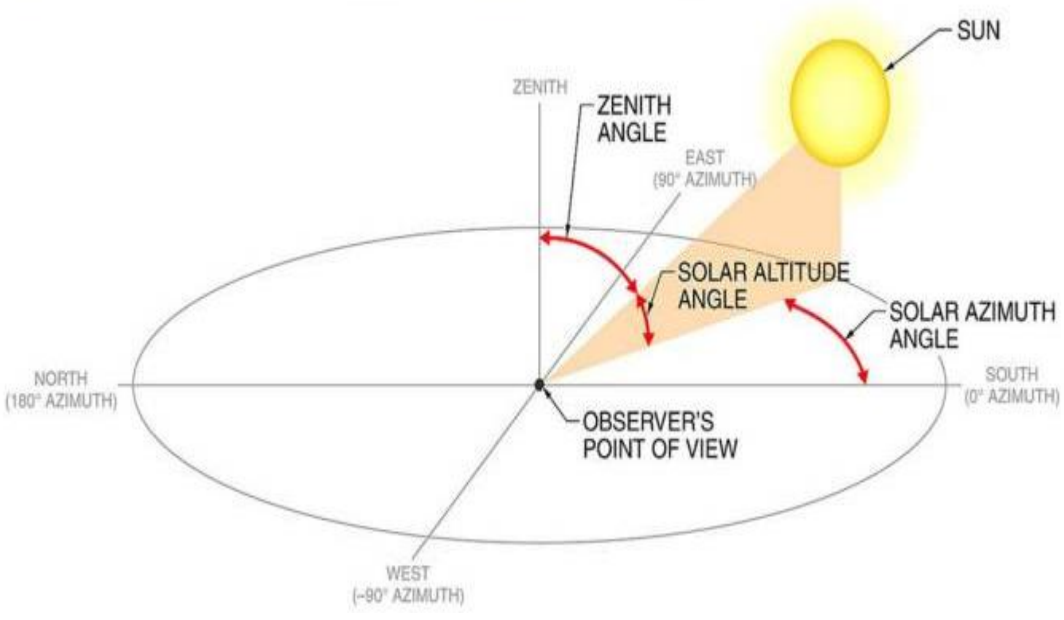

***Figure 3.2**: the Sun's altitude and azimuth angles*

3.3 Modeling of solar radiation on horizontal surface :

The radiation reaching the earth's surface can be signified in a number of different ways. Horizontal radiation (I_{TOT}) is the total amount of shortwave radiation received from above by a surface horizontal to the ground. This value is of specific interest to photovoltaic installations and includes both direct beam radiation (IB_H) and diffuse horizontal radiation (ID_H), which can be shown in equation below:

$$I_{TOT} = IB_H + ID_H \qquad (3.15)$$

Direct normal radiation or direct radiation is the amount of solar radiation received per unit area by a surface that is always perpendicular to the radiation that comes in a straight line from the direction of the sun at its current location in the sky. Usually, you can increase the amount of radiation that is received by the surface by keeping the surface perpendicular to the radiation upon arrival radiation.. This item can be expressed through

$$IB_H = I_B \sin\alpha \qquad (3.16)$$

Where I_B is direct beam which can be expressed by

$$I_B = Ae^{\frac{-k}{m}} \qquad (3.17)$$

Where A is an apparent extraterrestrial flux , K is a dimensionless factor called optical depth and m is an air mass. A, K and m factors can be expressed as functions of day number as follows

$$A = 1160 + 75\,\mathrm{sind}\left[\frac{360}{365}(N - 275)\right] \qquad (3.18)$$

$$k = 0.174 + 0.035 \operatorname{sind}\left[\frac{360}{365}(N - 100)\right] \quad (3.19)$$

$$m = \frac{1}{\sin\alpha} \quad (3.20)$$

On the other hand, Diffuse Horizontal Irradiance or diffuse radiation is the amount of radiation received per unit area by a surface that does not arrive at a direct path from the sun, but has been scattered by molecules and particles in the atmosphere and comes equally from all directions. Which can be approximated by:

$$ID_H = CI_B \quad (3.21)$$

Where C can be expressed as follow:

$$C = 0.095 + 0.04 \operatorname{sind}\left[\frac{360}{365}(N - 100)\right] \quad (3.22)$$

3.*4* Modeling of solar radiation in tilted surface:

In this case, the surface is tilted at a fixed angle, so to determine the quantity of solar radiation is done through a set of equations in addition to relying on some values that were calculated in this case of the horizontal surface, The radiation value can be expressed by the following equation:

$$IC_{TOT} = IB_C + ID_C + IR_C \quad (3.23)$$

The previous equation expresses three components of radiation, which means there is an additional type was not found in the case of the horizontal surface, which is the reflected radiation (IR_C).

Beam radiation, diffuse radiation and reflected radiation can be calculated by following equations depended on Liu and Jordan model:

A -Beam radiation: this is radiation can be calculated by:

$$IB_C = I_B \operatorname{cosd} \theta \tag{3.24}$$

Where θ is zenith angle;

Zenith Angle (θ) is the angle between the local zenith (i.e. directly above the point on the ground) and the line of sight from that point to the sun. And can be calculated by:

$$\operatorname{cosd} \theta = \operatorname{cosd} \alpha \ \operatorname{cosd}(\Phi_s) \operatorname{sind} \beta + \operatorname{sind} \alpha \operatorname{cosd} \beta \tag{3.25}$$

Where β is a tilt angle and in this case is fixed

Tilt angle of the photovoltaic (PV) is the key to an optimum energy yield. PV arrays are most efficient, when they are perpendicular to the sun's rays. The default value is a tilt angle equal to the station's latitude plus 15 degrees in winter or minus 15 degrees in summer.

On the other hand, noted there are two types of azimuth angle based on the reference, one for the collector (Φ_C) which means the angle of deviation direction of the collector from the south and equal zero. And the other for the sun (Φ_S) which means the angle of deviation direction of the sun rays due to the south and calculated Previously.

B- Diffuse radiation (ID_C):

Many models used to determine (ID_C) that can be classified into isotropic and anisotropic models. Isotropic model mean that radiates uniformly in all directions from a point source.

Liu and Jordan model one of isotropic models, which used in calculated of diffuse radiation in inclined surface, and presented in equation below:

$$ID_C = ID_H \frac{1+\cos\beta}{2} \tag{3.26}$$

C- Reflected radiation (IR_C): which is the amount of solar energy redirected from a surface, based on the solar reflectance or albedo of the surface material. Moreover, the value of IR_C can be find by using the following equation:

$$IR_C = \rho\, I_{TOT} \frac{1-\cos\beta}{2} \tag{3.27}$$

Where ρ is the albedo of the surface and it change based on the nature of the surface.

3.5 Modeling of solar radiation in tracking solar collector:

There are several types of solar tracking system, and here we will specialize in dual-axis solar tracker.

Dual-axis trackers allow solar panels to move in two directions instead of one, which means more energy from the sun due to the greater range of direction finding.Moreover, the energy consumption needed to move the solar tracker would also be greater than that used in other types.

In an attempt to get the largest amount of solar energy the solar tracker moves constantly to keep the solar radiation closer to perpendicular to the surface and therefore there are two angles remain variable because of the movement, namely azimuth and tilt angles. Which can be found in follow equations:

$$\Phi_C = \Phi_S \tag{3.28}$$

Where Φ_c is the azimuth angle of the collector and this angle keep equal to the azimuth angle of the sun.

In addition, tilt angle (β_1) can be expressed by the following equation:

$$\beta_1 = 90 - \alpha \tag{3.29}$$

Because of permanent change in tilt angle (β_1) dominated synchronous change on Zenith Angle (θ_t), which can be expressed in the following equation:

$$\text{cosd}\,\theta_t = \text{cosd}\,\alpha\ \text{cosd}(\Phi_s - \Phi_C)\,\text{sind}\,\beta_1 + \text{sind}\,\alpha\,\text{cosd}\,\beta_1$$

(3.30)

Now it is possible to find the value of solar radiation in the case of the tracker as shown in following equation:

$$IT_{TOT} = IB_T + ID_T + IR_T \tag{3.31}$$

Where IB_T is the beam radiation and can be calculated by using the following equation:

$$IB_T = I_B \operatorname{cosd} \theta_t \tag{3.32}$$

Moreover, ID_T is the diffuse radiation on tracking surface and can be expressed by the following equation:

$$ID_T = ID_H \frac{1+\cos\beta_1}{2} \tag{3.33}$$

Moreover, IR_T is the reflection radiation on tracking surface and can be expressed by the following equation:

$$IR_T = IR_H \frac{1-\cos\beta_1}{2} \tag{3.34}$$

3.6 Modeling algorithms of the sun trackers

The first algorithm displays the working mechanism used to determine the amount of production from solar radiation when the tracker is in the horizontal state during daylight hours.

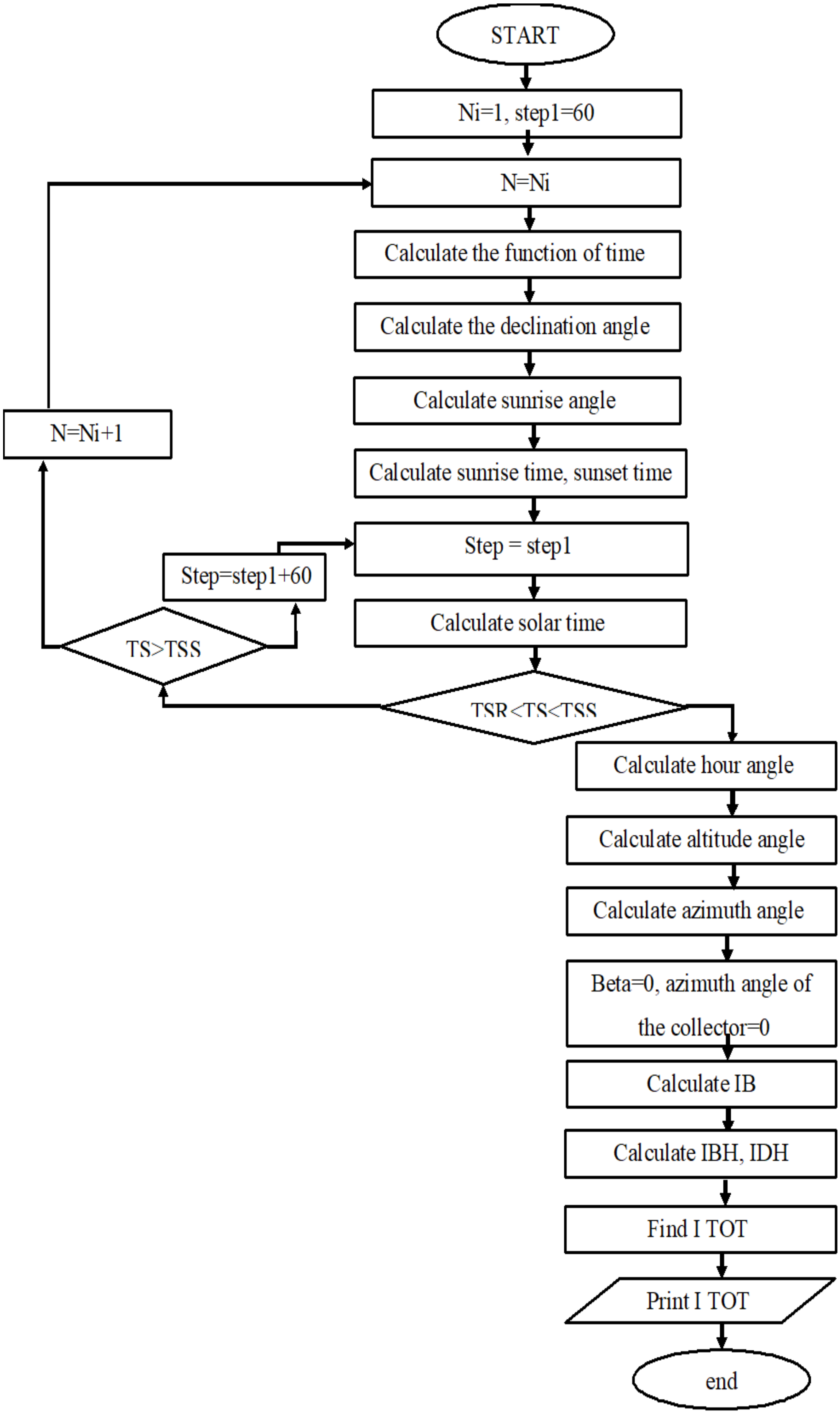
START
Ni=1, step1=60
N=Ni
Calculate the function of time
Calculate the declination angle
Calculate sunrise angle
Calculate sunrise time, sunset time
Step = step1
Calculate solar time
TSR<TS<TSS
Calculate hour angle
Calculate altitude angle
Calculate azimuth angle
Beta=0, azimuth angle of the collector=0
Calculate IB
Calculate IBH, IDH
Find I TOT
Print I TOT
end
TS>TSS
Step=step1+60
N=Ni+1

While the second algorithm, depending on the first algorithm, displays the working, mechanism of the solar tracker when it is fixed at a beta angle to find the amount of solar radiation produced during daylight hours.

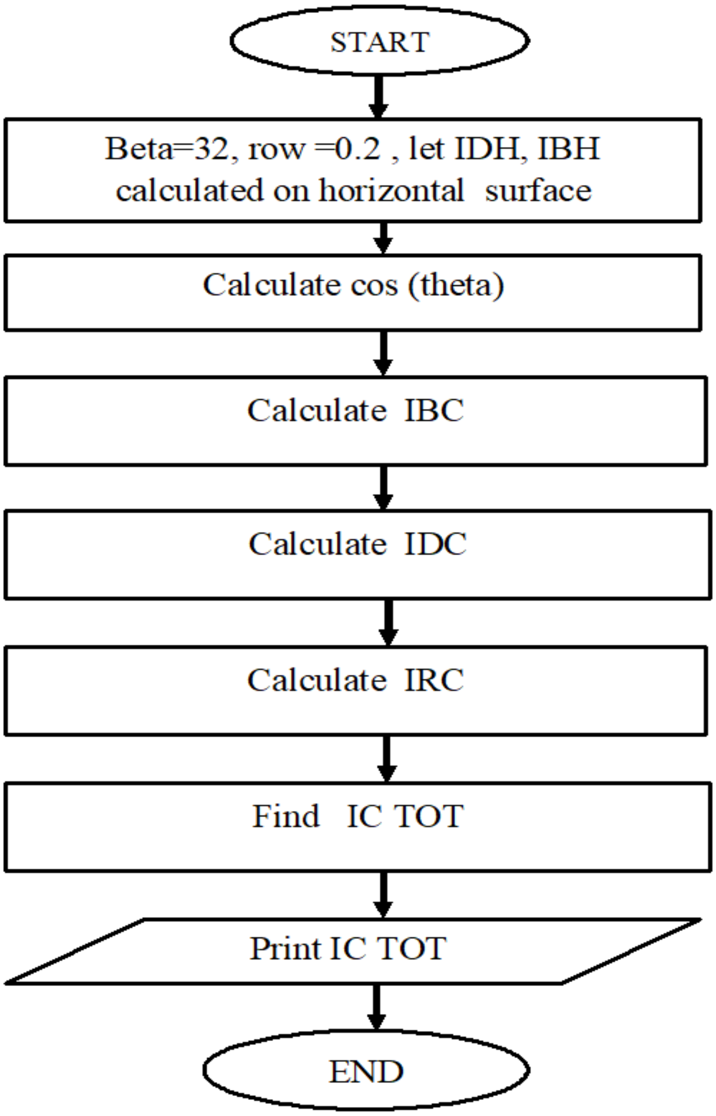

In the last algorithm, it displays the model of the two-axis solar tracker, based on the first algorithm, when it is $\Phi_s = \Phi_c$ to determine the amount of production from the solar ray during daylight hour.

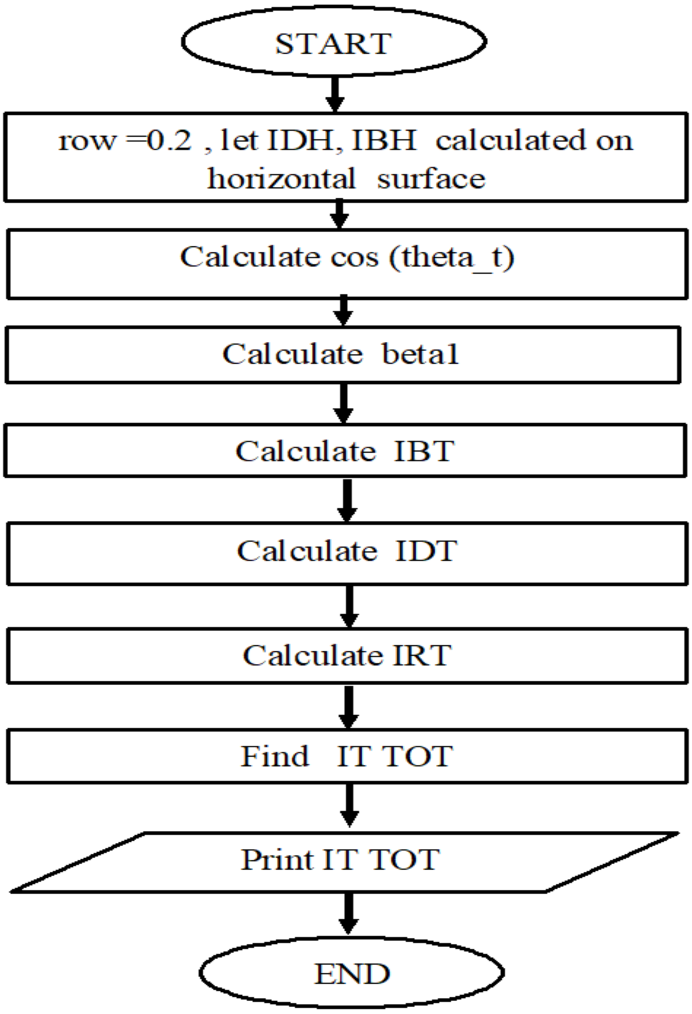

3.7 Modeling of sun trackers:

The sun tracking system that lets PV panel orthogonal to the sun radiation during the day, can raise the focused sun radiation by up to 40%. The fixed tracker cannot generally track the sun trajectory, also the single-axis tracking system can follow the sun in the horizontal direction (azimuth angle), while the two-axis tracker tracks the sun path in both azimuth and altitude angles. Dual axis automated control-tracking system, which tracks the sun in two planes (azimuth and altitude) to move a system to the direction of ray diffusion of sun radiation. The designed tracking system constructed of microcontroller or programmable logic control (PLC) with a digital program that operates sun tracker using driver, gearbox to control the angular speed and mechanical torque, supports and mountings. Stepper motor is modelled to attendant the panel perpendicular to the sun's beam.

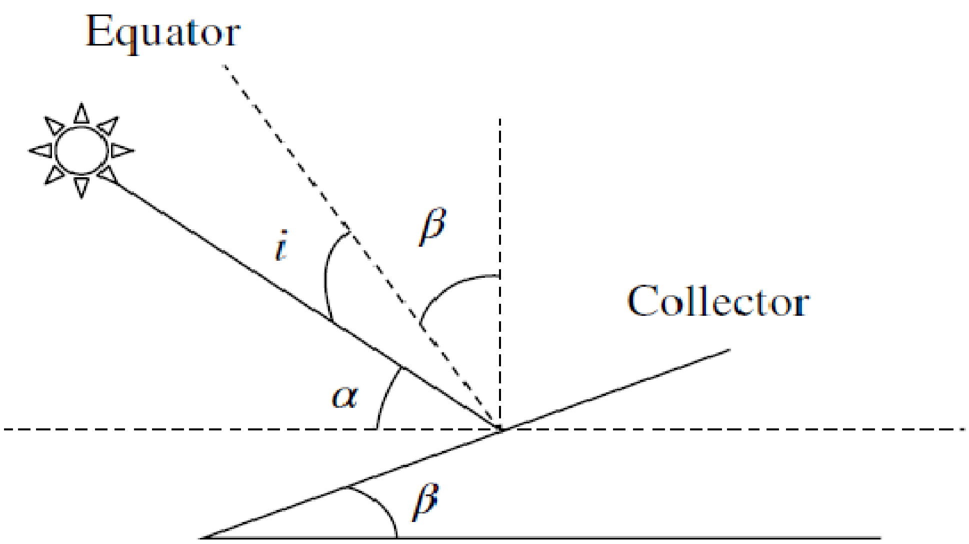

***Figure 3.3**: geometrical angles of sun's projection*

From the Earth's perspective, the Sun is moving across the sky during the day. The above figure shows the principle of dual axis Sun tracker. The perpendicular path between the Sun projection and the collector is called the equator. The angle between the collector and the reference line is called tilt angle (β), and the angle between the Sun projection and the collector is called altitude angle (α). The incident angle (i) is the angle between the Sun projection and the equator. The maximum power can be achieved at a tilt angle, which considers a zero incidence angle. The relationships of the tilt, altitude, and incidence angles are given in the following:

At AM time,

$$\beta + \alpha - i = 90 \tag{3.35}$$

And at PM time,

$$\beta + \alpha + i = 90 \tag{3.36}$$

To achieve the maximum radiation by the collector, the incidence angle (i) must be zero, and so the optimum tilt angle can be determined as follows:

$$\beta = 90 - \alpha \tag{3.37}$$

Chapter four

Results analyses

The analysis of the results obtained using a method to predict the amount of solar radiation absorbed from different systems is the most important step to verify the goal of the study, which is to know the effectiveness of the solar energy tracker in increasing energy production throughout the summer. Beginning of analyzing the results of the horizontal solar system, the solar system with the angle of inclination and the dual axis solar tracker system, then all results are compared to find out the most efficient systems in terms of electrical energy output. As all the systems used depend on one production period, which is the period from sunrise to sunset, with a rate of change every hour during the period. It should be noted that the results presented are based on Assuming that summer is ideal over the entire period, because of using the clear sky model to predict solar radiation values. Before starting the analysis of the monthly results for the summer season, the following two tables present the absorbed solar radiation and the electrical energy produced based on the radiation for the three models within one day to be a model for each month. It is worth noting that any energy losses from the inverter , the cables and the effect of heat on the panel have been neglected, and the system capacity of 2 kW_p has been dealt with.

Table 4.1: daily solar radiation absorbed by solar collectors

month	Day NO.	Working hours	Horizontal collector	Tilted collector	Tracking collector
June	156	15	9.915	10.233	16.363
July	186	15	9.917	10.227	16.262
August	217	14	9.447	9.599	15.327
September	248	13	8.554	9.172	14.660

Table 4.2: daily electrical energy produced by solar collectors

month	Day NO.	Worki ng hours	Horizontal collector	Tilted collector	Tracking collector
June	156	15	20.820	21.490	34.361
July	186	15	20.830	21.477	34.150
August	217	14	19.840	20.160	32.186
September	248	13	17.963	19.262	30.790

The following graphs present a comparison between the three models in terms of solar radiation and the output of electrical energy.

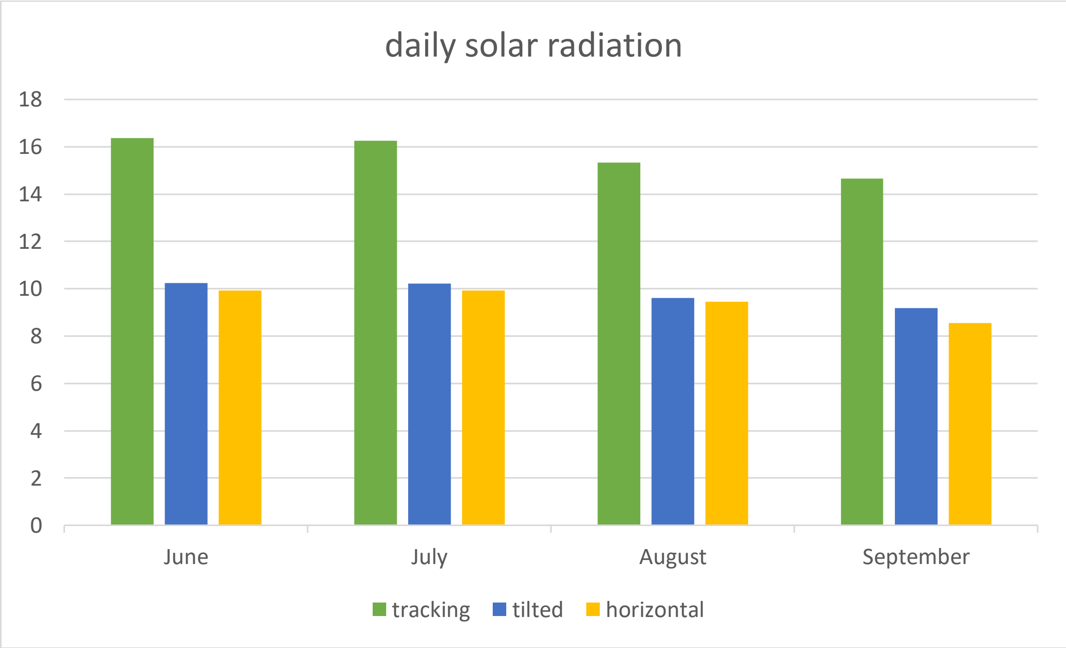

Figure 4.1**:** *Daily comparison between the three solar collectors in terms of solar radiation*

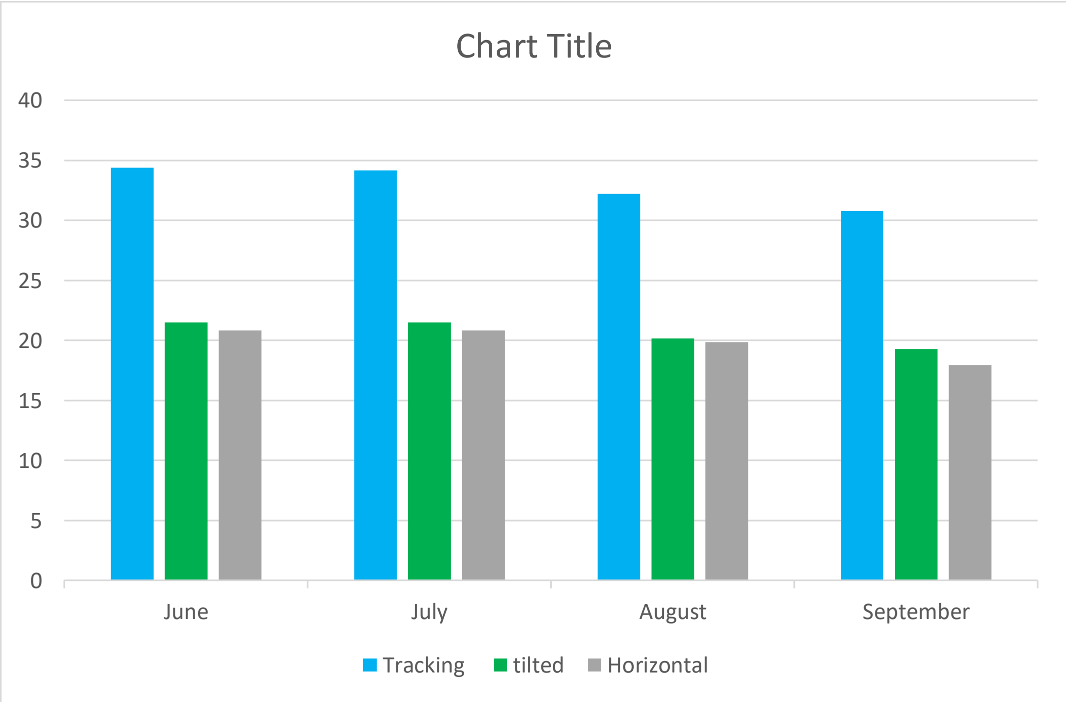

Figure 4.2: *Daily comparison between the three solar collectors in terms of electrical energy***.**

Followed by dealing with the three systems of the economic aspect of judgment, which models were the most abundant, and thus we determine if the use of the solar tracker achieved all the advantages in terms of productivity and economic savings.

4.1 Results on horizontal surface:

When looking at the results, the amount of solar radiation in the horizontal solar collector

ranged between (243.93 - 301.33 kW / m2 per month), with the highest absorption of solar radiation during August and the lowest level in September, as shown in Table (4.3).

The table below shows the number of daylight hours during each month, the rate of solar radiation during the day, and the amount of energy produced in the summer season.

Table 4.3: the results of horizontal surface system

Month	**Work hours (h)**	**Monthly radiation (kW/m2)**	**Monthly average radiation(kW/m2) per hour**	**Monthly Energy production (kWh)**
June	447	297.9	0.666442953	625.59
July	442	301.33	0.681742081	632.79
August	424	283.86	0.669481132	596.11
September	380	243.93	0.641921053	512.26

The figures (4.3) & (4.4) show the monthly solar radiation and monthly energy production depending on the data shown in the previous table.

Based on Figure (4.3), it is clear that there is a slight difference in solar radiation during June and July, then it begins to decrease somewhat during August and September.

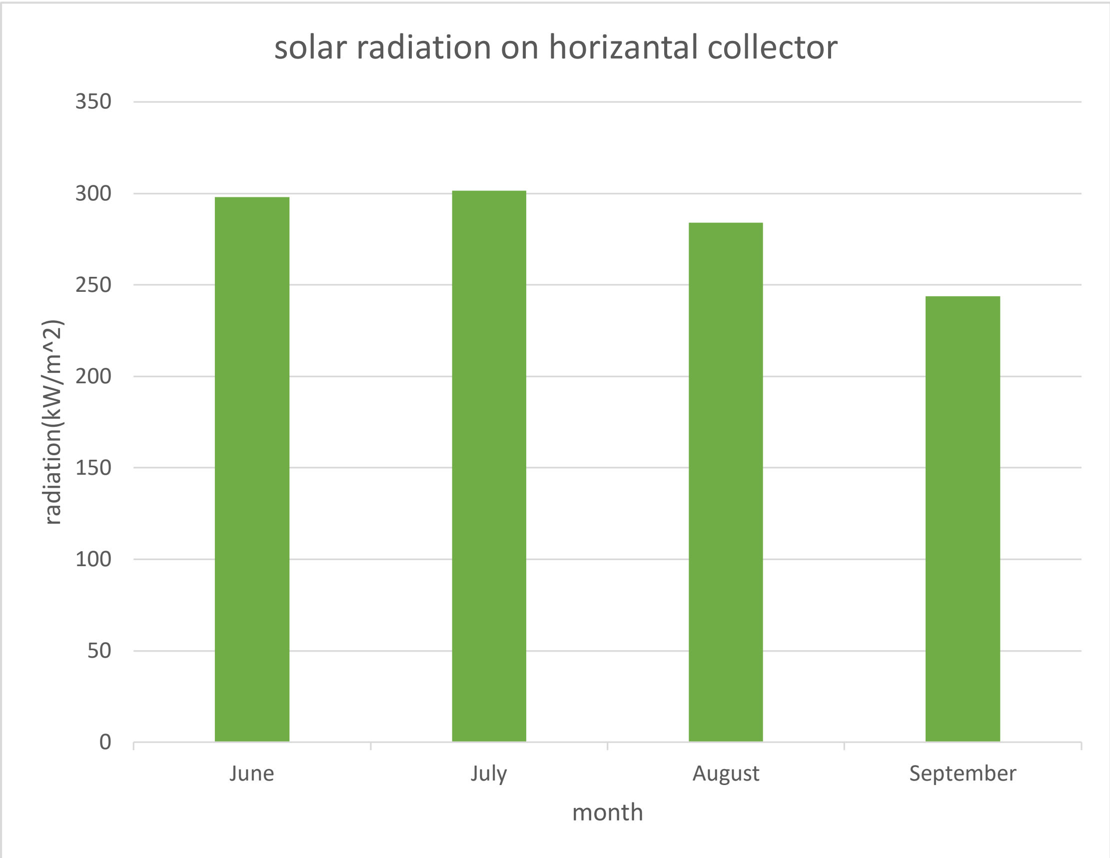

Figure 4.3: *Monthly distribution of solar radiation on a horizontal solar system*

Since the production of energy depends on the amount of solar radiation. We find that the greater amount of radiation from the sun, the amount of energy produced increases. This is evident in the following picture, which shows that the production of energy was the largest during the summer months One of the most important factors that played in the difference for energy produced from month to others, which is the number of working hours for the system that was associated with the number of daylight hours that range from sunrise to sunset.

In addition, the position of the solar panels horizontally has a significant impact on production. The production recorded the highest value at noon when the rays are perpendicular to the solar panels.

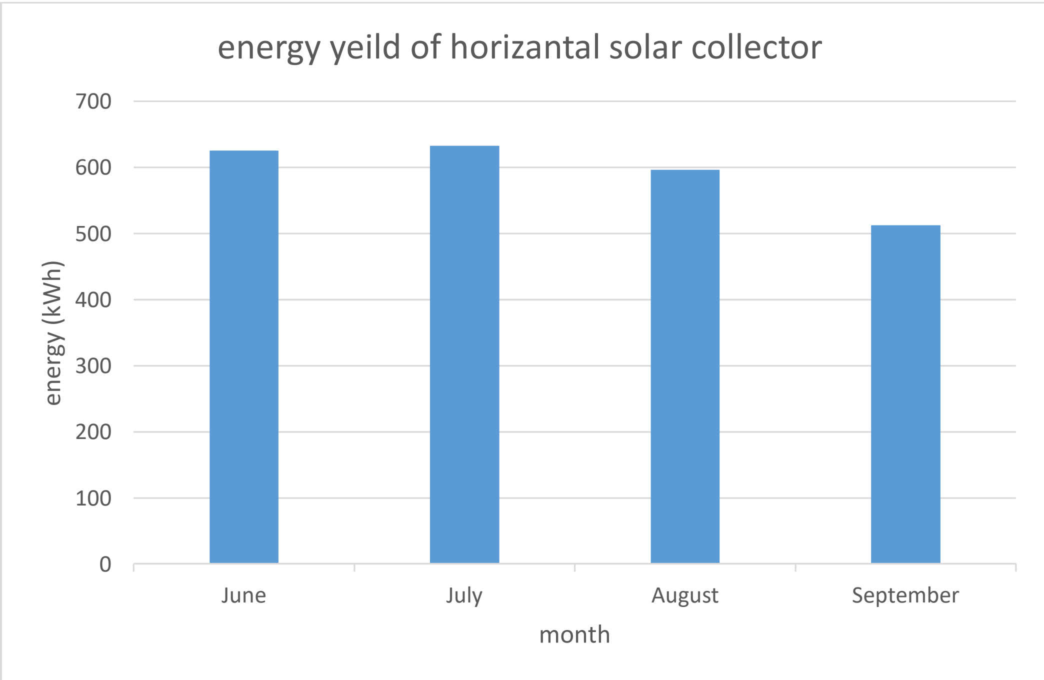

Figure 4.4 *: Monthly distribution of energy produced by solar system fixed horizontally*

Figures (5.a, 5.b) show the hourly distribution of solar radiation during the summer months. As it seems, the highest value of solar radiation was during July, and this value was recorded on most days during the month at noon.

The matter was no different in June in terms of values of absorbed solar radiation, but working hours decreased slightly.

As for August and September, there is a decrease in working hours and the values of absorbed solar radiation, so the production of electrical energy from the solar system begins to decrease .

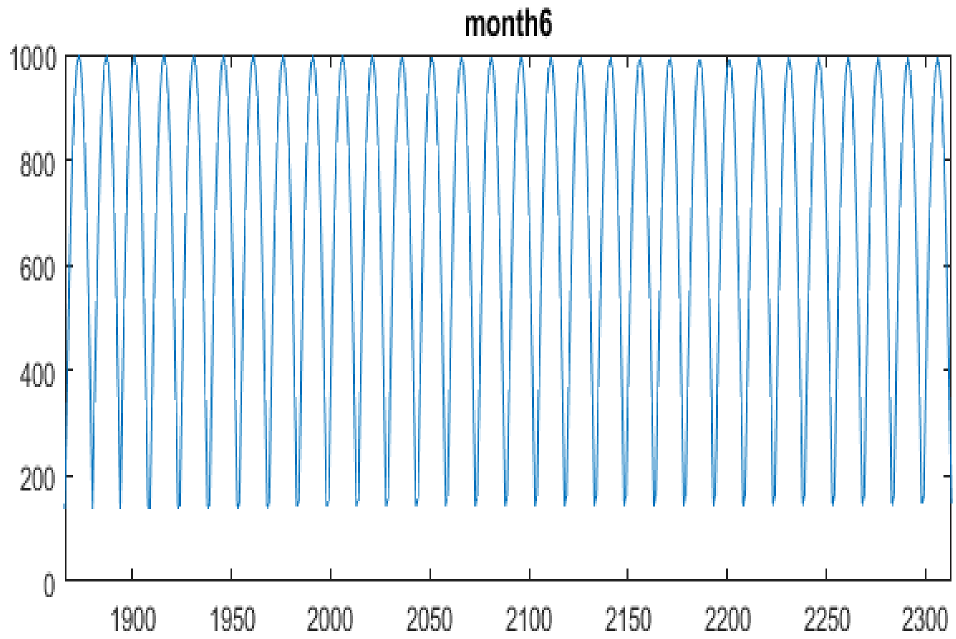

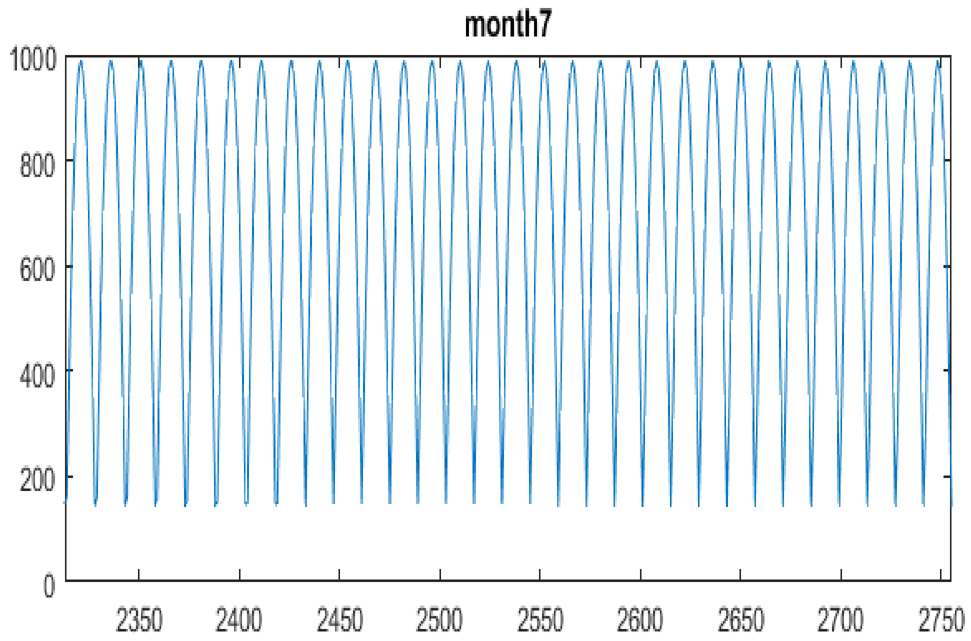

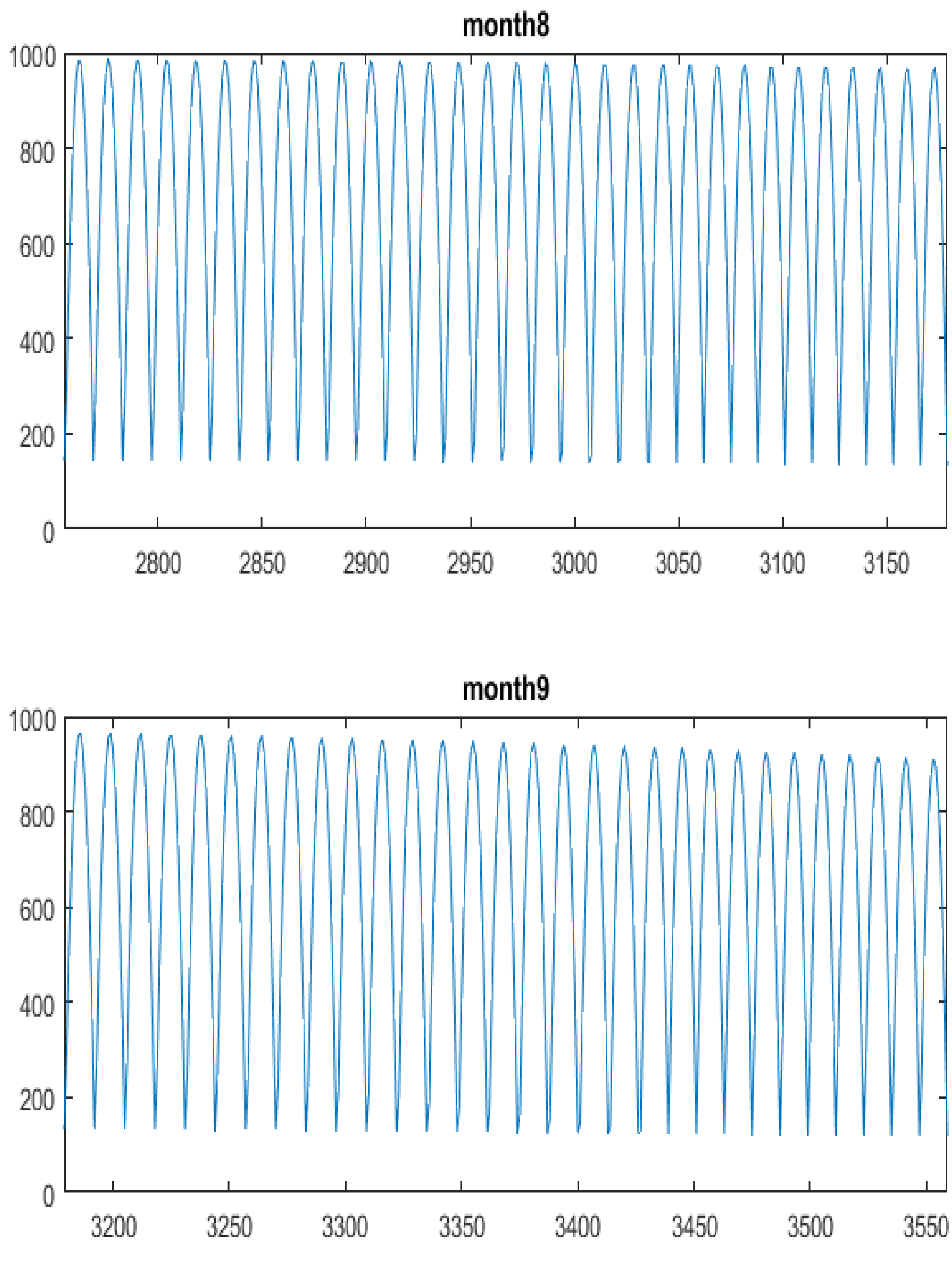

Figure 4.5: *(a) The hourly distribution of solar radiation on horizontal solar system during June and July (b) The hourly distribution of solar radiation on horizontal solar system during August and September.*

4.2 Results of tilt surface:

After reviewing the results of the horizontal solar collector, Now it is required to analyze the results of the second system, which is the tilted solar collector.

These results include solar radiation during daylight hours, and the amount of energy produced from this radiation as shown in table (4.5).

After focusing on the results, the amount of solar radiation during the summer months ranging between 274.98 kWh /m2 and 306.47 kWh /m2.

Table (4.4): the results of tilted surface system

Month	Work hours (h)	Monthly radiation (kW/m2)	Monthly average radiation (kW/m2)	Monthly energy production (kWh)
June	447	306.47	0.68562	643.58
July	442	305.65	0.69152	641.86
August	424	292.2	0.68915	613.4
September	380	274.98	0.72363	577.46

These values in the previous table are represented by a chart as shown in the figures (4.6) & (4.7):

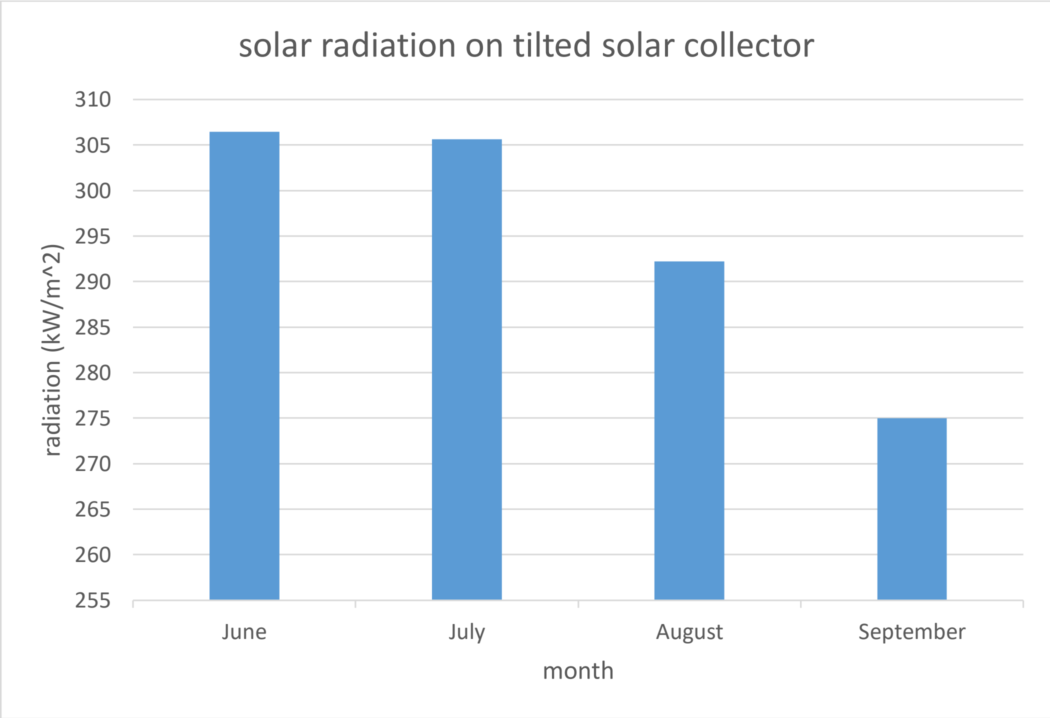

Figure 4.6: *Monthly distribution of solar radiation on a tilted solar system*

It appears from the previous figure that the change was somehow different, but it was the largest summer radiation during the months of June and July.

It is clear from the figure (4.7) the amount of energy produced by the sun's rays, which have a direct relations with each other, so, we note that the distribution of production of energy throughout the summer season is very similar to the distribution of solar radiation.

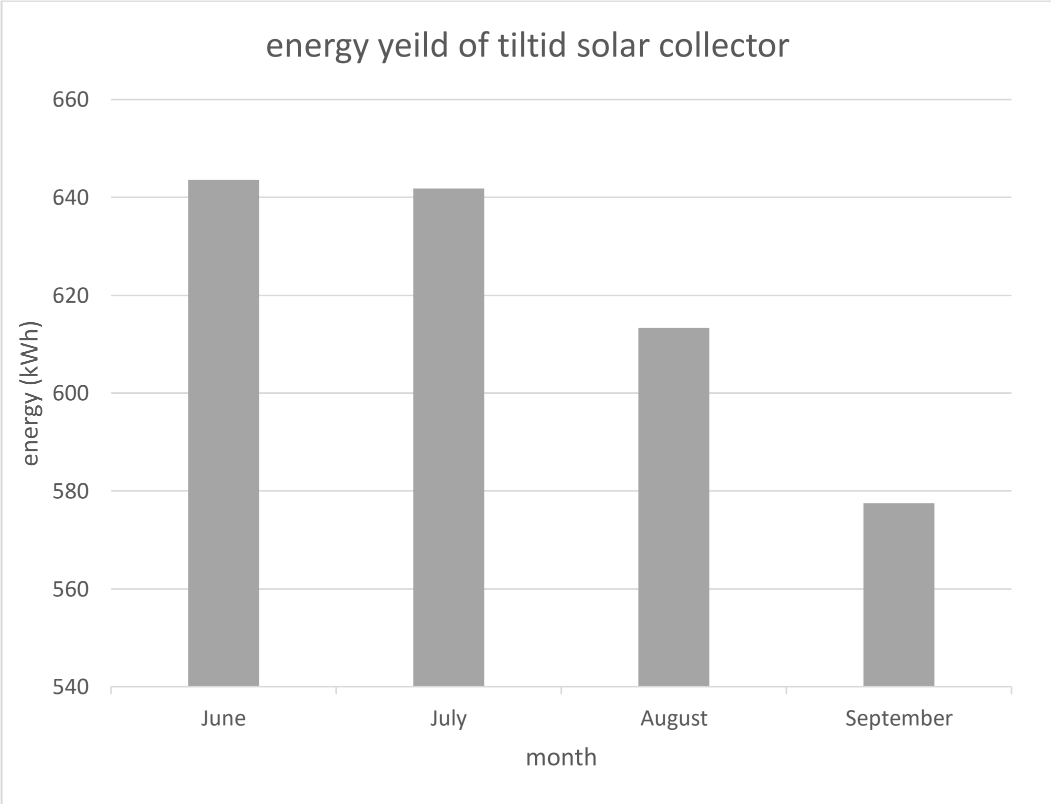

Figure 4.7: *Monthly distribution of energy produced by tilted solar system*

In Addition to that, the figures (8.a,8.b) show the hourly distribution of solar radiation during the summer months, So that the hours that record the highest solar radiation appear during the day of every month, and thus the best time to produce electrical energy.

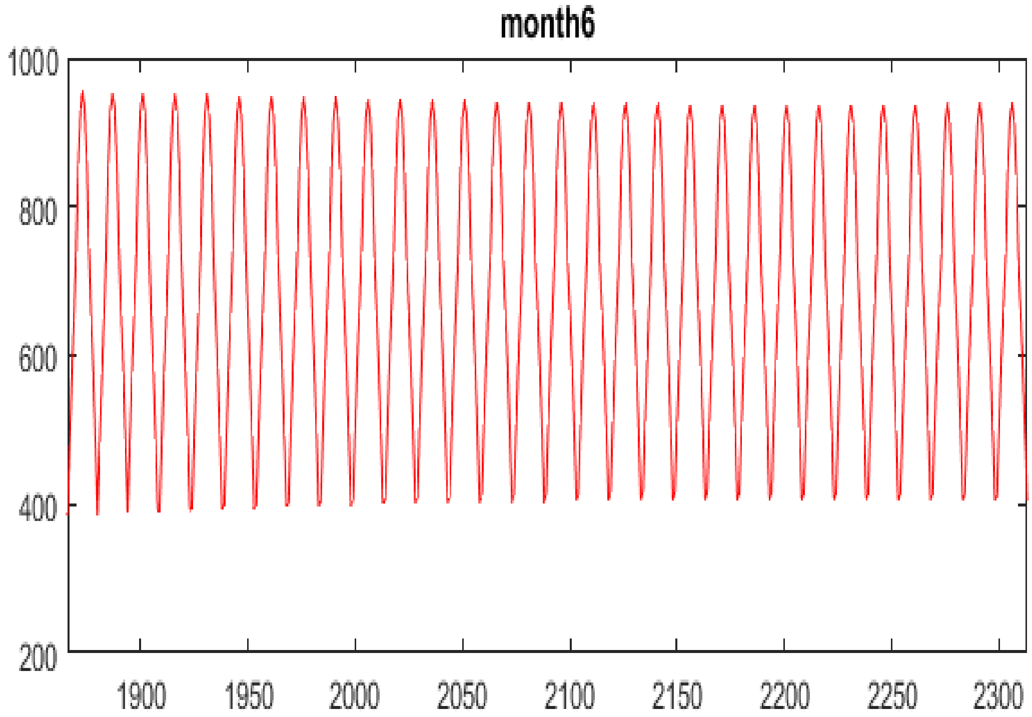
month6
1000
800
600
400
200
1900
1950
2000
2050
2100
2150
2200
2250
2300

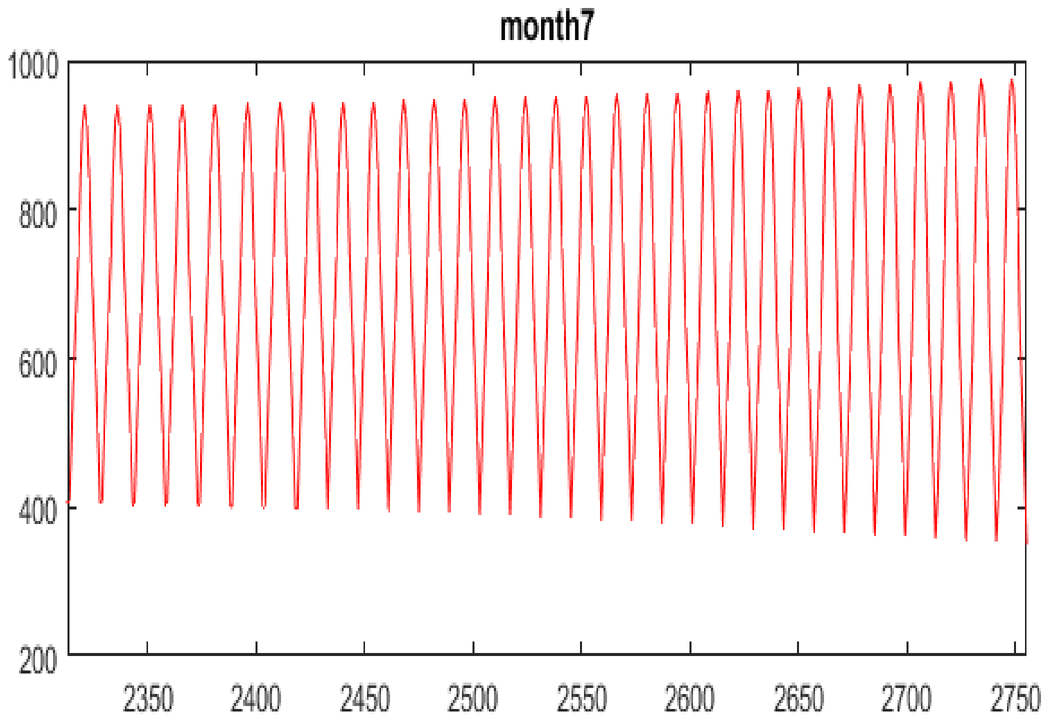
month7
1000
800
600
400
200
2350
2400
2450
2500
2550
2600
2650
2700
2750

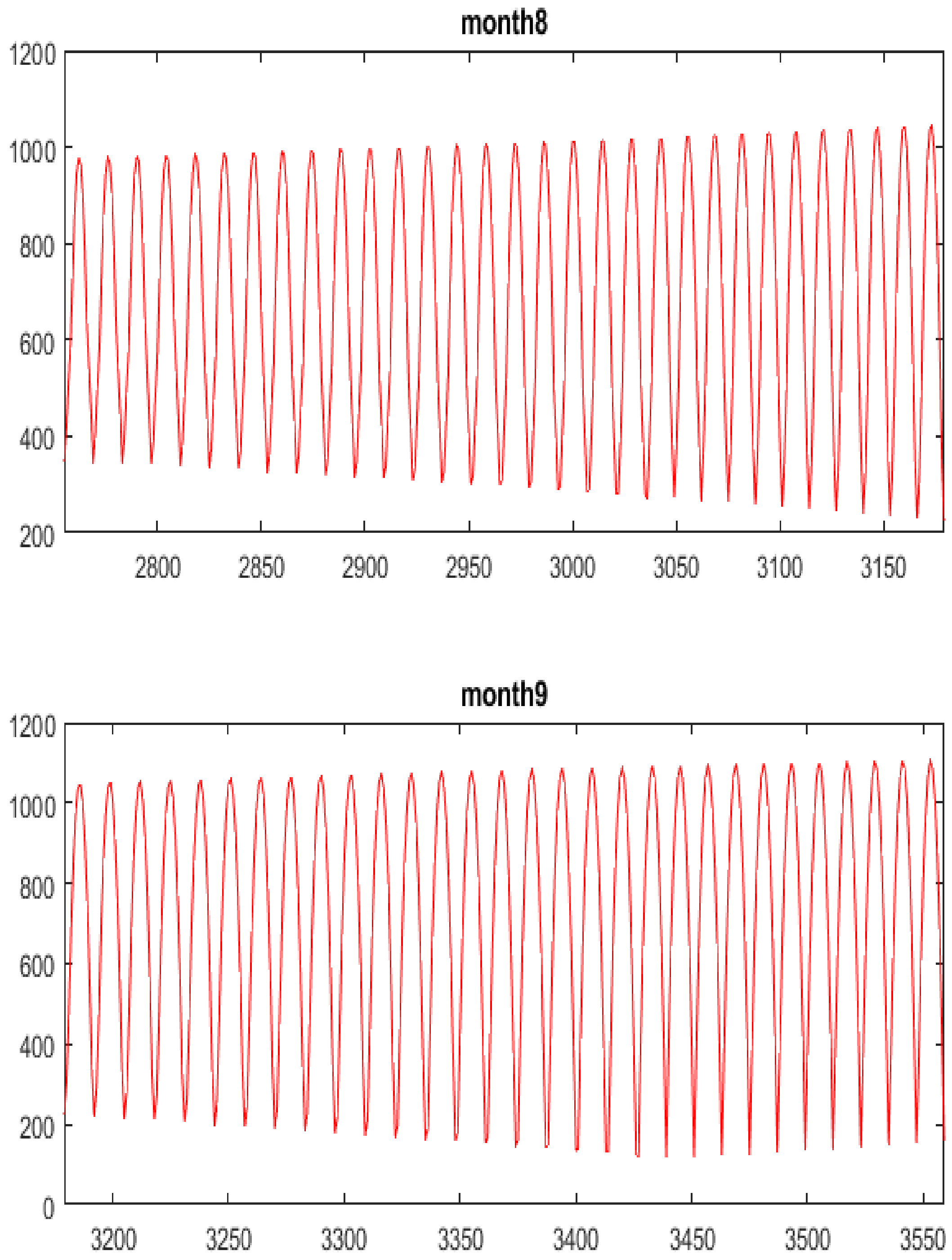

Figure 4.8: *(a) The hourly distribution of solar radiation on tilted surface during June and July (b) The hourly distribution of solar radiation on tilted surface during August and September.*

4.3 Results of tracking solar collector:

In this section, we are going to analyze the results obtained using the dual axis tracker to see if it is feasible to use compared to systems installed horizontally or installed at a tilt angle.

In the table (4.5), notice the presence of another element, namely, the amount of energy used by the motor in the dual axis solar tracker, in addition to the amount of energy produced, the amount of radiation.

The dual-axis solar tracker consumes electrical energy when it moves, estimated at 125 watts per hour. This value was adopted through the information contained in the data sheet for these solar trackers as it contains a motor that moves the system every hour based on the change of the sun’s position in the sky during daylight hours.

This system works during the daylight hours of every month. It is determined from the sunrise hour to the sunset hour. Therefore, the amount of energy consumed per month was calculated using the following equation:

$$\text{consuption energy} = \text{work hour No.} \times \text{hourly consumption energy} \tag{4.1}$$

$$\text{consuption energy} = \text{work hour No.} \times 0.125\text{kWh} \tag{4.2}$$

for example, in June

$$\text{consuption energy} = 447 \times 0.125 = 55.88\text{kWh}$$

Likewise, it continues to count for the remaining months of the summer season.

Table (4.5): the results of duel axis tracker system

Month	Work hours (h)	Monthly radiation (kW/m2)	Monthly average radiation (kW/m2)	Monthly energy production (kWh)	energy consumption (kWh)	Final energy (kWh)
June	447	485.56	1.086264	1019.7	55.875	963.825
July	442	478.99	1.083688	1005.9	55.25	950.65
August	424	468.56	1.105094	983.97	53	930.97
September	380	434.17	1.142553	911.76	47.5	864.26

Note that the values of solar radiation range from (434.17-485.56(kW/m^2)) to be the highest radiation in June, and the lowest in September , this is also reflected for energy produced.

As for the energy consumed by the tracker, we notice that it depends on the number of working hours of the system to be the highest consumption during June and the lowest in February.

The figures (4.9) & (4.10) shows a graphical representation of the amount of solar radiation and the amount of energy produced shown in the previous table.

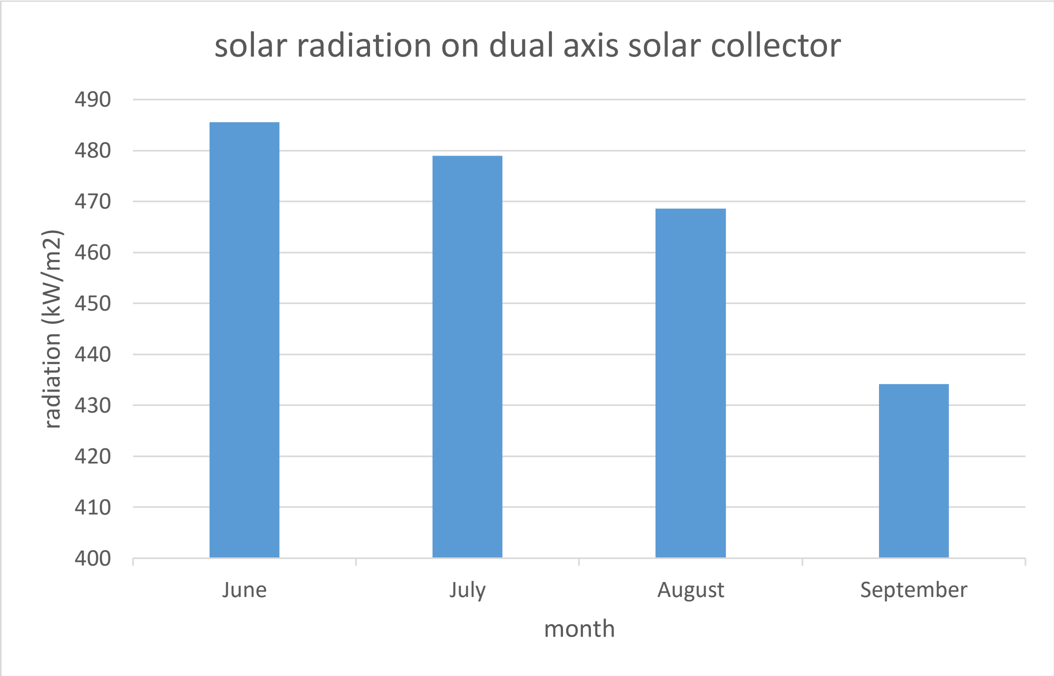

Figure 4.9*: Monthly distribution of solar radiation on a tracking solar system*

It is clear from the figure (4.9) that the amount of radiation received through the solar tracker system is concentrated in the same region, whether in summer or winter, with a slight difference in value to be higher during the month of June, May and July.

The matter is not very different when checking the graphical representation in the figure (4.10) for the amount of produced energy, as it is a reflection of the solar radiation curve in terms of the monthly distribution of production.

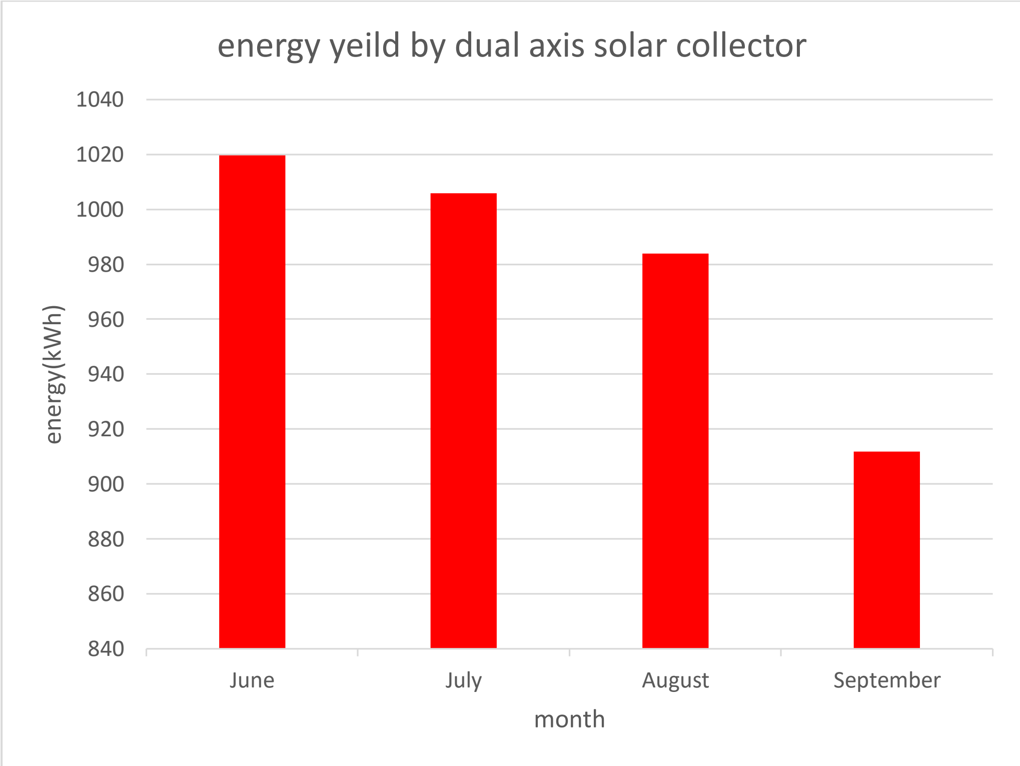

Figure 4.10: *Monthly distribution of energy produced by tracking solar system*

The following figure shows the monthly distribution of the energy consumed by the system in summer season, which is used a part of the energy produced by the system, where is the remaining part of the this is the final energy for use in different forms.

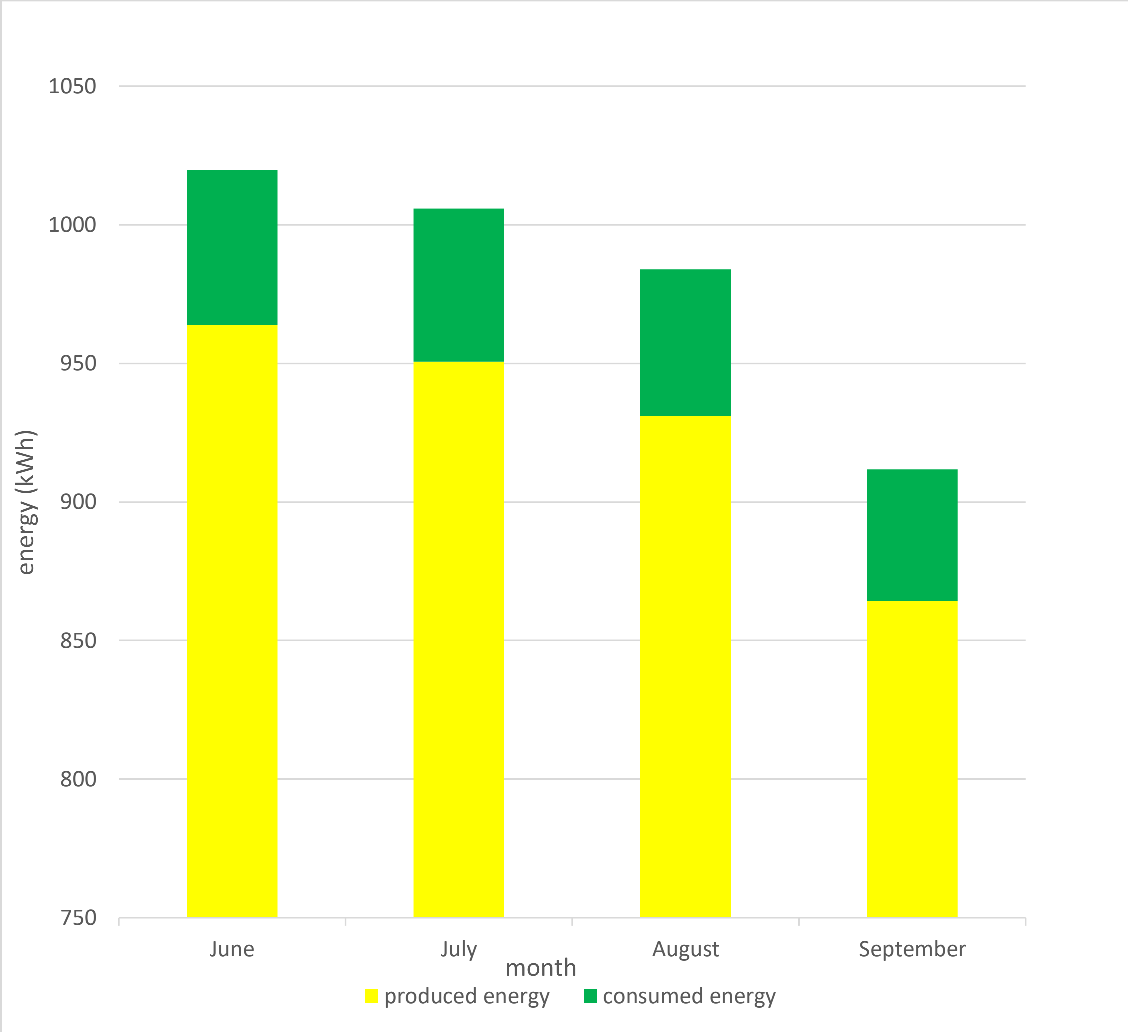

Figure 4.11: *Monthly distribution of energy produced and consumption by tracking solar system*

After reviewing the monthly results of solar radiation and the energy produced through the dual axis tracked system, it is necessary to clarify the distribution of solar radiation during working hours to show the highest value of solar radiation during daylight hours, as shown in the figure (12.a,12.b).

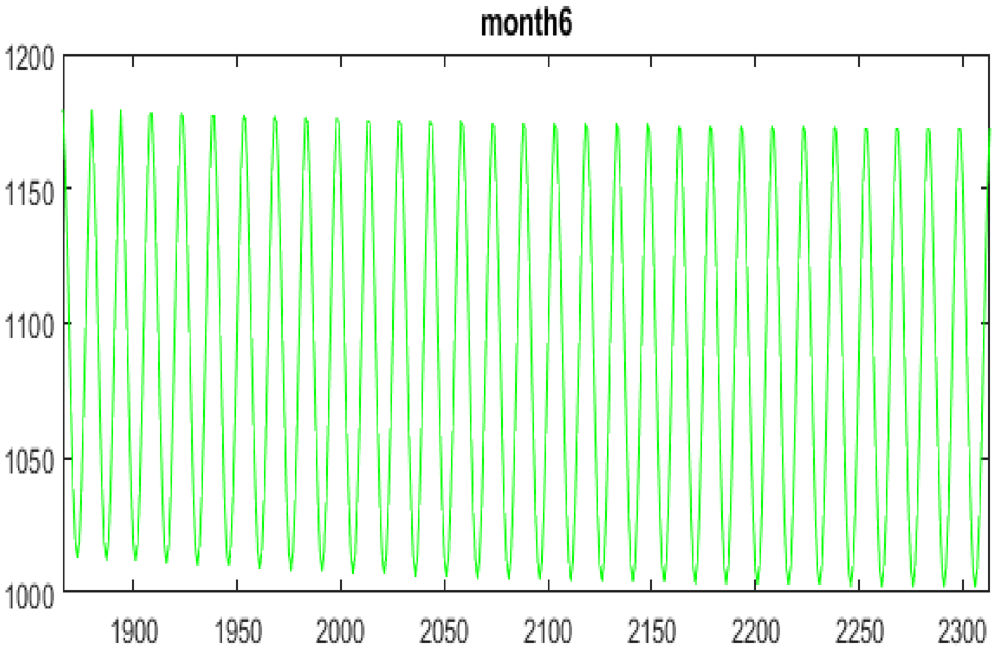
month6
1200
1150
1100
1050
1000
1900
1950
2000
2050
2100
2150
2200
2250
2300

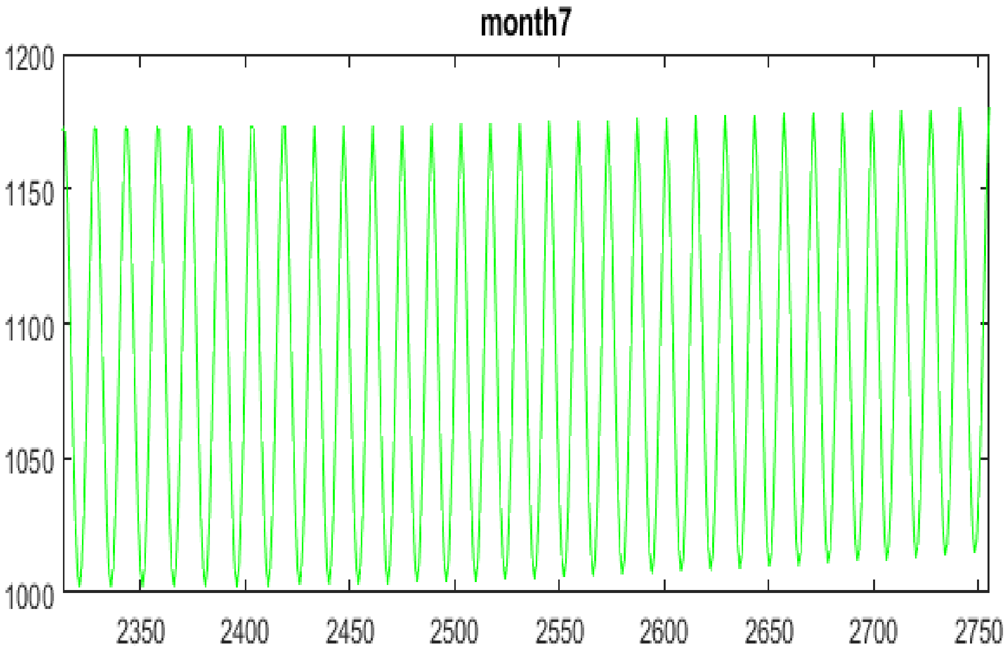
month7
1200
1150
1100
1050
1000
2350
2400
2450
2500
2550
2600
2650
2700
2750

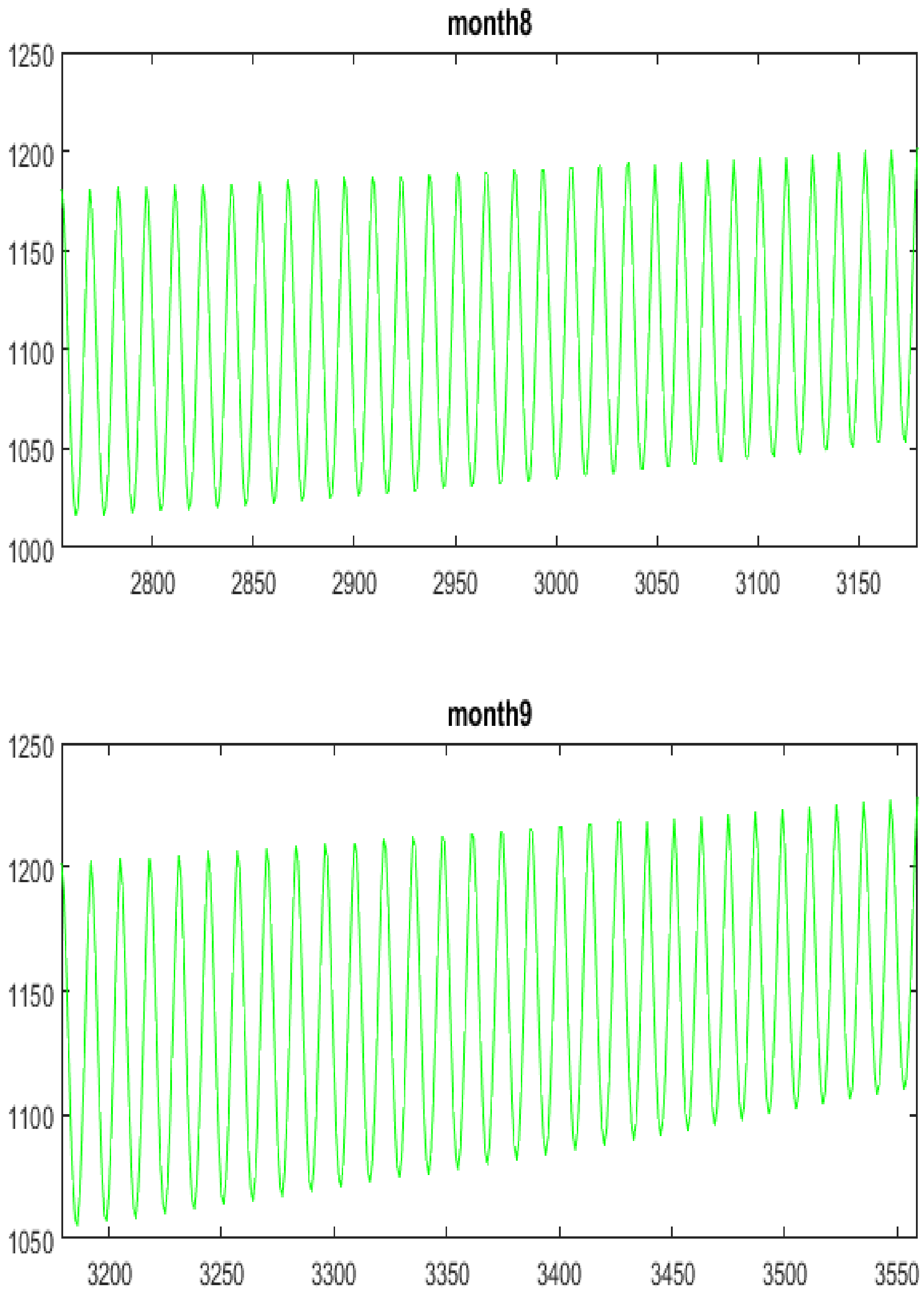

Figure 4.12*: (a) The hourly distribution of solar radiation on tracking solar system during June and July (b) The hourly distribution of solar radiation on tracking solar system during August and September.*

After checking the results, a strong convergence of the solar radiation values was observed during the working hours of the summer months, as they ranged between 1000 and 1190 kilowatts per square meter, and thus the high radiation value was recorded during the summer period, which increases the productivity of electrical energy.

4.4 Comparison of systems

After analyzing all the results for each solar system separately, it is necessary to compare them to determine which systems are better than their energy production.

The following table shows the monthly values of solar radiation for the three systems, through which it is clear that the highest results were in the favor of the system that contains a dual-axis solar tracker, this reflects that the energy produced will be the highest.

While the values are converging for the two systems tilted solar collector and horizontal solar collector .

Table 4.6: Comparison of systems in term of radiation

Month	work hour	radiation dual axis (kW/m2)	Radiation on tilt surface (kW/m2)	Radiation horizontal (kW/m2)
June	447	485.56	306.47	297.9
July	442	478.99	305.65	301.33
August	424	468.56	292.2	283.86
September	380	434.17	274.98	243.93

The figure (4.13) shows the graphical representation of the values in the previous table, to make it more clearly about the difference in the monthly values of solar radiation.

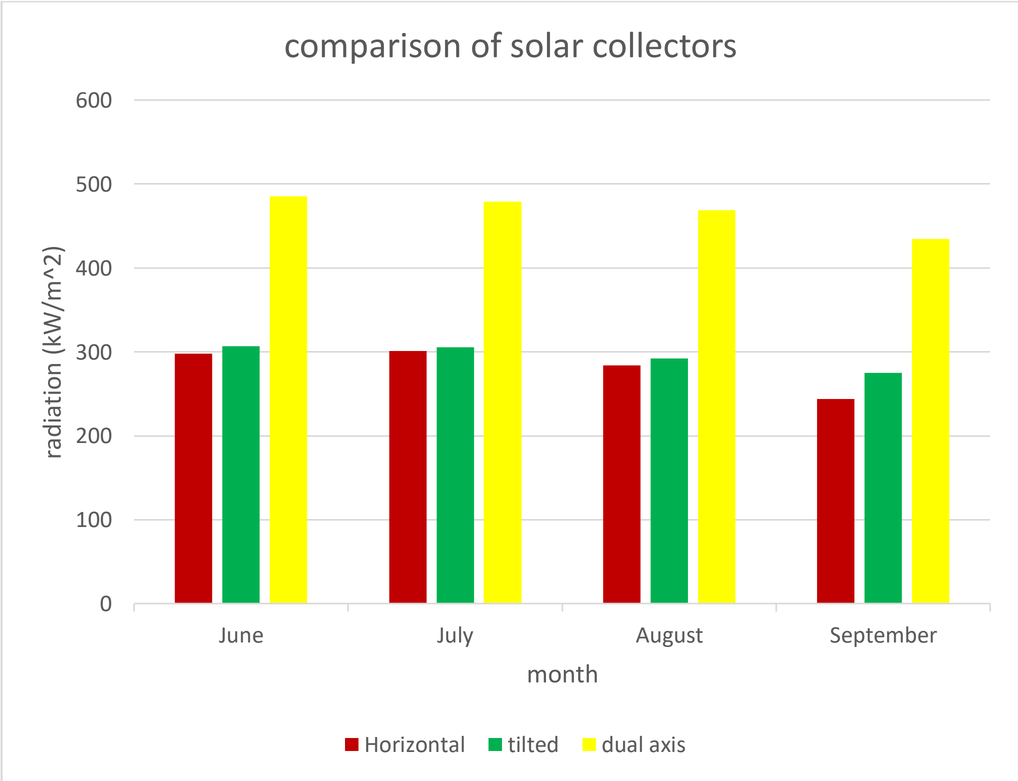

***Figure 4.13**: Monthly comparison of the three systems in terms of solar radiation*

The most important thing in the comparison is to know which systems are more productive and this is what can be observed through the table (4.7) that contains the monthly production of energy in addition to the amount of energy used by the dual-axis tracker.

After looking at the following table, it shows clearly the difference in energy production using the tracker compared to the other two systems, Also, the amount of energy the tracking system consumes compared to the product is very small.

Table 4.7: Comparison of systems in term of energy

month	wok hour (h)	Ene g consum tion by dual axis tracker (kWh)	Energy pr duced by dal axis tracker (kWh)	final ener-gy of dual axis track-er (kWh)	Energy pr duced by tilt surface (kWh)	Energy produce by horizon-talsurface (kWh)
June	447	55.875	1019.7	963.825	643.58	625.59
July	442	55.25	1005.9	950.65	641.86	632.79
August	424	53	983.97	930.97	613.4	596.11
September	380	47.5	911.76	864.26	577.46	512.26

The following figure shows the graphical distribution of energy production from the three systems based on the values mentioned in the previous comparison table.

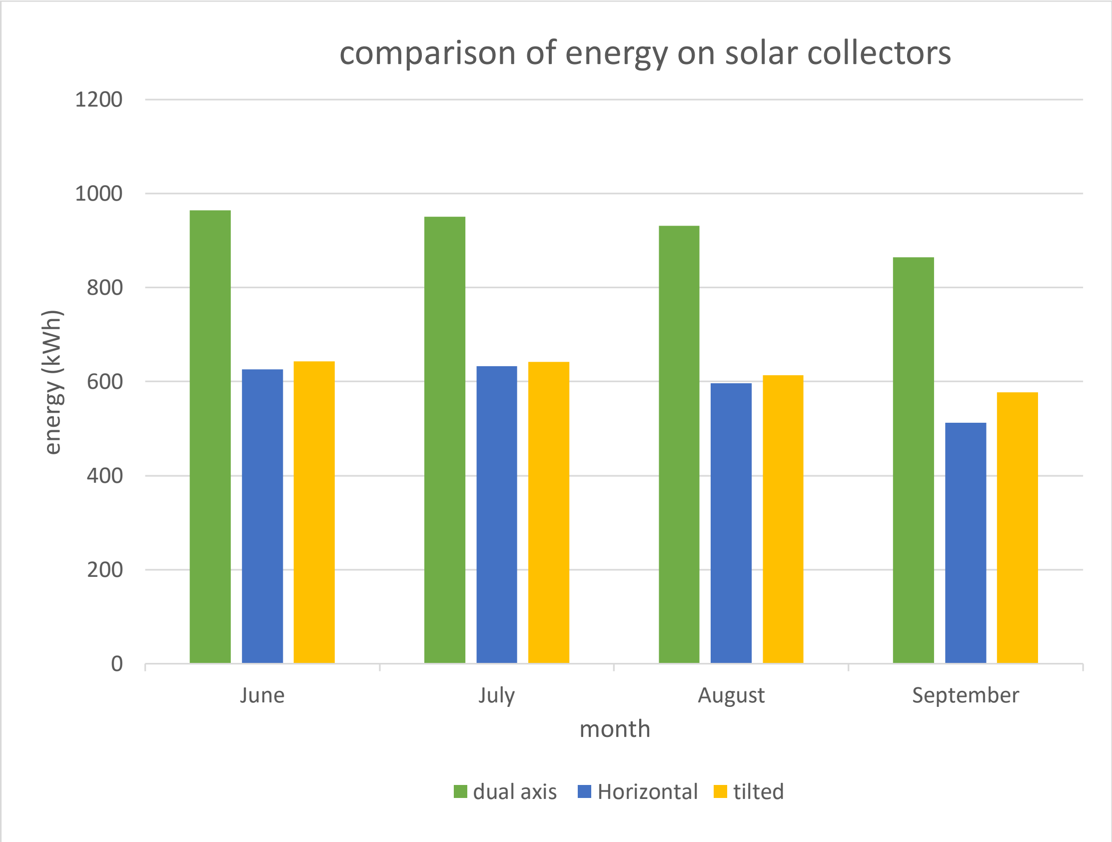

Figure 4.14: *Monthly comparison of the three systems in terms of solar radiation*

Despite the high effectiveness of the solar tracking system in terms of energy production, however this is not the only factor that makes the dual-axis tracking system superior to all other systems.

Chapter five

Economic analysis of fixed, tilted and tracked Solar collector systems

After completing the analysis of the results related to the three systems in terms of the amount of solar radiation absorbed and the amount of electrical energy produced, accordingly, it was found that the tracking system of the solar collector is the most efficient, but this axis cannot be satisfied in the comparison, as there is another axis of great importance, which is the economic aspect.

Therefore, make a comparison between the three systems using one of the economic viability methods.

5.1 Cost of energy method:

The cost of energy or COE is similar to the concept of the payback for energy systems. However, instead of measuring how much is needed to recoup the initial investment, the COE determines how much money must be made per unit of electricity (kWh, MWh etc. or even other type of energy like home heating) to recoup the lifetime costs of the system. This includes the initial capital investment, maintenance costs, the cost of fuel for the system (if any), any operational costs and the discount rate.

The COE is one way of determining whether a firm will build a project because if the project will not break even then it will not be built. The COE is a useful tool because it can combine both the fixed costs and variable costs into a single measurement to simplify analysis. To determine the COE, a firm will determine the necessary parameters such as the lifetime of the system, how much electricity it will produce and the input costs. The formula is:

$$COE = \frac{\text{Total cost of ownership (\$)}}{\text{System production over its lifetime (kWh)}} \qquad (5.1)$$

After adopting this method to determine the economic feasibility of each of the three systems. The necessary information for making the calculations must be provided, including the cost of the system, its life cycle, the maintenance and operation cost of the system over its life cycle and benefit from the amount of electrical energy produced that was previously calculated . In the matter of determining the cost of the three systems, many solar energy companies have been contacted to find out the prices in the local markets, and price offers for the fixed and tracked system were obtained as shown in Appendices D and F.

Based on what was mentioned in the price offer, the following table displays the cost of constructing a fixed solar collector in its two states, horizontal, tilted, and dual axis tracking solar collector, and the annual cost of monitoring and maintenance the systems as presented in Maintenance contract from one of the companies operating in this field .

Table 5.1: Financial information about solar collector systems

Type of the collector	**Initial price ($2kW_p$)**	**Annual Maintenance price**
Horizontal solar collector	2181$	400$
Tilted solar collector	2181$	400$
Tracking solar collector	4481$	500$

The following table shows the energy produced by each system in order to use in calculation of cost of energy.

Table 5.2: Energy production of the solar collector systems

Type of the collector	**Energy production in summer season**
Horizontal solar collector	2366.75kWh
Tilted solar collector	2476.30kWh
Tracking solar collector	3709.71kWh

5.2 cost of energy calculation:

By using the Cost of Energy equation and the information provided in the previous tables to find the price of a kilowatt hour and find out which systems are the lowest.

For horizontal solar collector:

$$COE = \frac{\text{inetial cost}+(\text{M\&O}\times\text{LC})}{\text{annual energy production (kWh)}\times\text{LC}} \quad (5.2)$$

$$COE = \frac{2181\$+(400\times25)}{2366.75\times25} = 0.206\$/kWh \quad (5.3)$$

For tilted solar collector:

$$COE = \frac{2181\$+(400\times25)}{2476.30\times25} = 0.197\$/kWh \quad (5.4)$$

For tracking solar collector:

$$COE = \frac{4481\$+(500\times25)}{3709.71\times25} = 0.183\$/kWh \quad (5.5)$$

Based on the results obtained, it was proved that the solar tracking system achieved the lowest price per kilowatt-hour among the three solar collectors systems.

Chapter sex

Conclusion and future work

The most important thing is extracted from the current study that focuses on the comparison between solar collector systems installed in three ways, the first is horizontally, the second is tilted by angle, and the last is a dual-axis solar tracker; in terms of the amount produced by the electric energy based on the solar radiation absorbed by the cells in summer season to find that they are consecutive respectively as follows 2366.75kWh , 2476.30kWh, 3709.71kWh. It becomes clear through these values of productivity that the dual-axis solar tracker worked to increase the effectiveness of photovoltaic systems, Where it worked to increase the productivity of electric power compared with the productivity of the other two systems, horizontal and inclined at an angle, and this is an advantage in favor of the tracker.

On the other hand, which is the economic side, the solar tracker proved to be the most economical, as despite its high price in its construction, it was the lowest price per kilowatt hour among the three systems, where the horizontal, inclined and tracker systems recorded the following prices respectively$0.206/kWh , 0.197$/kWh , and 0.183$/kWh.

The current study was conducted by relying on clear sky modeling, as this modeling could not be adopted throughout the year. Therefore, the work was limited to predicting solar radiation and the consequent production of electrical energy during the summer period, and the study was based on time and for a date without taking into account the change that may occur in the atmosphere. Such as the emergence of clouds and the difference in the intensity of radiation. Therefore, one of the resigned work is to design the solar collectors in their three states and take readings and compare the practical results with theory to support the conclusion.

References

- Fathabadi H. **Novel high accurate sensor less dual-axis solar tracking system controlled by maximum power point tracking unit of photovoltaic systems**. App l Energy 2016; 173:448–59. http://dx.doi.org/10.1016/j.apenergy.2016.03.109.
- Hong T, Jeong K, Ban C, Oh J, Koo C, Kim J, et al. **A preliminary study on the 2-axis hybrid solar tracking method for the smart photovoltaic blind**. Energy Procedia 2016 ;88:484–90. http://dx.doi.org/10.1016/j.egypro.2016.06.067.
- Maia CB, Ferreira AG, Hanriot SM. **Evaluation of a tracking flat-plate solar collector in Brazil**. Appl Therm Eng 2014;73:953–62. http://dx.doi.org/10.1016/j. applthermaleng.2014.08.052.
- Gholinejad M, Bakhtiari A, **Bidi M. Effects of tracking modes on the performance of a solar MED plant**. Desalination 2016;380:29–42. http://dx.doi.org/10.1016/j. desal.2015.11.015.
- Seme S, Stumberger G**. A novel prediction algorithm for solar angles using solar radiation and differential evolution for dual-axis sun tracking purposes**.Sol Energy 2011;85:2757–70. http://dx.doi.org/10.1016/j.solener.2011.08.031.
- Wei X, Lu Z, Yu W, Zhang H, Wang Z. **Tracking and ray tracing equations for the target-aligned heliostat for solar tower power plants.** Renew Energy 2011;36:2687–93. http://dx.doi.org/10.1016/j.renene.2011.02.022.

- Ferdaus RA, Mohammed MA, Rahman S, Salehin S, Abdul Mannan M. **Energy efficient hybrid dual axis solar tracking system.** J Renew Energy 2014:1–12. http://dx.doi.org/10.1155/2014/629717.

- Zogbi R, Laplaze D**. Design and construction of a sun tracker**. Sol Energy1984;33:369–72. http://dx.doi.org/10.1016/0038-092X(84)90168-3.

- Rumala S-SN. **A shadow method for automatic tracking.** Sol Energy1986;37:245–7. http://dx.doi.org/10.1016/0038-092X(86)90081-2.

- Das S, Chakraborty S, Sadhu PK, Sastry OS. **Design and experimental execution of a microcontroller (μC)-based smart dual-axis automatic solar tracker.** Energy Sci Eng 2015;3:558–64.

- Bentaher H, Kaich H, Ayadi N, Ben Hmouda M, Maalej A, Lemmer U. **A simple tracking system to monitor solar PV panels.** Energy Convers Manag 2014;78:872–5. http://dx.doi.org/10.1016/j.enconman.2013.09.042

- Parmar NJ, Parmar AN, Gautam VS. **Passive solar tracking system.** Int J Emerg Technol Adv Eng 2015;5:138–45.

- Chia-Yen Lee, Po-Cheng Chou, Sun Tracking Systems, A review. Sensors 9 (2009): 3875-3890

- H. Mousazadeh, A. Keyhani, **A review of principle and sun-tracking methods for maximizing solar systems output**. Renewable and Sustainable Energy Reviews RSER-656 (2009).

- M. Yakup, A.Q. Malik**, Optimum tilt angle and orientation for solar collector in Brunei Darussalam**. Renew. Energy. 24 (2001):223-234.

- S. Bari, **Optimum slope angle and orientation of solar collectors for different periods of possible Utilization**. Energy Convers. Manage, 41(2000): 855-860.

- Society, T. G. S. E., **Planning and Installing Photovoltaic Systems**, Ecofys (2005).

Appendices:

Appendix A:

```
%% Location of Nablus, L=(32.13), LOD =(35.16)

clc

clear all

L = 32.13 ; %Latitude

LOD = 35.16 ; %Longitude

T_GMT = +3 ; % time diffrent with referance to GMT

step = 60 ; % time step

Ni=[];

I_TOTf=[];

DSi=[];

p1=[];

for N=365:-1:1

    Ni=[N;Ni];

DS = 23.45*(sind((360.*(N-81)./365))) ; %angle of declination

 DSi=[DS;DSi];
```

```
B = (360.*(N-81))/364 ;% equation of time

EOT = ((9.87.*sind(2*B)) - (7.53.*cosd(B))-(1.5.*sind(B))); %equa-
tion of time

LTM  = 15*T_GMT ;%local time meridian

if LOD >= 0

    TS_correction = (-4*(LTM - LOD))+ EOT ; % solar time correction

else

     TS_correction = (4*(LTM - LOD))+ EOT ; % solar time correction

end

Hsr_i = -tand(DS)*tand(L); % sun rise hour angle

Hsr = acosd(Hsr_i); %sun rise angle

STSR = abs(((Hsr/15)-12)*60); % sunrise solar time

STSS = abs(((Hsr/15)+12)*60); % sunset solar time

TSR = STSR + abs(TS_correction ); %actual time of sun rise

TSS = STSS + abs(TS_correction ); %actual time of sun set

sin_alpha_d = [];

Hsd=[];
```

```
for LMT=TSS : -step :TSR    %% for loop for the day time

    TS = LMT + TS_correction ;  %solar time

    HS = (15*(TS - (720)))./60 ; % hour angle degree

    sin_alpha_i = (sind(L).*sind(DS))+(cosd(L).*cosd(DS).*cosd(HS));
%altitude angle

    alpha = asind (sin_alpha_i);

    sin_alpha_d =[sin_alpha_i;sin_alpha_d];

    Hsd=[HS;Hsd];

end

sin_alpha_d;

alpha_d=asind(sin_alpha_d);

Hsd;

for i=length(sin_alpha_d):-1:1

alpha_d = asind(sin_alpha_d);

% % % %........ solar radiation calculation in horizantal surface

 A= 1160+(75*sind((360/365)*(N-275))); %solar energy flux

 K= 0.174+(0.035*sind((360/365)*(N-100))); %k is a factor
```

```
 C= 0.095+(0.04*sind((360/365)*(N-100))); %c is a factor

 m =(1./sin_alpha_d(i)); %air mass

 I_B =A.*exp(-K./m);%availabe beam radiation in the sky

 IB_H =I_B.*( sin_alpha_d(i));%collected beam by collector in hori-
zantal surface

 ID_H = C.*I_B ; %diffuse on horizantal surface

 I_TOT =IB_H+ID_H ; %total radiatin

 I_TOTf=[I_TOT;I_TOTf];

 p_H =  ((I_TOT./1000).*(6*350));

 p1 =[ p_H ; p1];

end

end

I_TOTf;

subplot(2,3,1)

plot(I_TOTf)

title ('month1')

subplot(2,3,2)
```

```
plot(I_TOTf)

title ('month2')

subplot(2,3,3)

plot(I_TOTf)

title ('month3')

subplot(2,3,4)

plot(I_TOTf)

title ('month4')

subplot(2,3,5)

plot(I_TOTf)

title ('month5')

subplot(2,3,6)

plot(I_TOTf)

title ('month6')

subplot(2,3,1)

plot(I_TOTf)

title ('month7')
```

```
subplot(2,3,2)

plot(I_TOTf)

title ('month8')

subplot(2,3,3)

plot(I_TOTf)

title ('month9')

subplot(2,3,4)

plot(I_TOTf)

title ('month10')

subplot(2,3,5)

plot(I_TOTf)

title ('month11')

subplot(2,3,6)

plot(I_TOTf)

title ('month12')

x_1=sum(I_TOTf)

E_1=sum(p1)
```

Appendix B:

```
%% Location of Nablus, L=(32.13), LOD =(35.16)

clc

clear all

L = 32.13 ; %Latitude

LOD = 35.16 ; %Longitude

T_GMT = +3 ; % time diffrent with referance to GMT

step = 60 ; % time step

Ni=[];

IC_TOTf=[];

DSi=[];

p2=[];

for N=365:-1:1

    Ni=[N;Ni];

DS = 23.45*(sind((360.*(N-81)./365))) ; %angle of declination

 DSi=[DS;DSi];

B = (360.*(N-81))/364 ;% equation of time
```

```
EOT = ((9.87.*sind(2*B)) - (7.53.*cosd(B))-(1.5.*sind(B))); %equa-
tion of time

LTM  = 15*T_GMT ;%local time meridian

if LOD >= 0

    TS_correction = (-4*(LTM - LOD))+ EOT ; % solar time correction

else

     TS_correction = (4*(LTM - LOD))+ EOT ; % solar time correction

end

Hsr_i = -tand(DS)*tand(L); % sun rise hour angle

Hsr = acosd(Hsr_i); %sun rise angle

STSR = abs(((Hsr/15)-12)*60); % sunrise solar time

STSS = abs(((Hsr/15)+12)*60); % sunset solar time

TSR = STSR + abs(TS_correction ); %actual time of sun rise

TSS = STSS + abs(TS_correction ); %actual time of sun set

sin_alpha_d = [];

Hsd=[];

for LMT=TSS : -step :TSR    %% for loop for the day time
```

```
        TS = LMT + TS_correction ;  %solar time

        HS = (15*(TS - (720)))./60 ; % hour angle degree

        sin_alpha_i = (sind(L).*sind(DS))+(cosd(L).*cosd(DS).*cosd(HS));
%altitude angle

        alpha = asind (sin_alpha_i);

        sin_alpha_d =[sin_alpha_i;sin_alpha_d];

        Hsd=[HS;Hsd];

    end

    sin_alpha_d;

    alpha_d=asind(sin_alpha_d);

    Hsd;

    for i=length(sin_alpha_d):-1:1

    alpha_d = asind(sin_alpha_d);

       %=======================on tilt an-
gle================================

     A= 1160+(75*sind((360/365)*(N-275))); %solar energy flux

     K= 0.174+(0.035*sind((360/365)*(N-100))); %k is a factor

     C= 0.095+(0.04*sind((360/365)*(N-100))); %c is a factor
```

```
m =(1./sin_alpha_d(i)); %air mass

I_B =A.*exp(-K./m);%availabe beam radiation in the sky

IB_H =I_B.*( sin_alpha_d(i));%collected beam by collector in hori-
zantal surface

ID_H = C.*I_B ; %diffuse on horizantal surface

I_TOT =IB_H+ID_H ; %total radiatin

beta = 32; % tilt angle

sin_PHI_Si =((sind(Hsd(i)).*cosd(DS))./cosd(alpha_d(i)));%azimuth
angleIB_H

PHI_S = asind(sin_PHI_Si);%azimuth angle

cos_theta =
((cosd(alpha_d(i))*cosd(PHI_S)*sind(beta))+(sind(alpha_d(i)
)*cosd(beta)));%zineth angle

theta = acosd (cos_theta); %zineth angle

IB_C = I_B.*(cos_theta) ;%collected beam by collector in tilt sur-
face

ID_C = ID_H .*((1+cosd(beta))./2); %diffuse on tilt surface

ROW = 0.2 ; % factor of reflection
```

```
IR_C = ROW.*(I_TOT).*((1-cos(beta))./2); %reflection on tilt sur-
face

IC_TOT =IB_C +ID_C +IR_C ;

IC_TOTf=[IC_TOT;IC_TOTf];

 p_c =  ((IC_TOT./1000).*(6*350));

p2 =[ p_c ; p2];

end

end

subplot(2,3,1)

plot(IC_TOTf,'red')

title ('month1')

subplot(2,3,2)

plot(IC_TOTf,'red')

title ('month2')

subplot(2,3,3)

plot(IC_TOTf,'red')

title ('month3')
```

```
subplot(2,3,4)

plot(IC_TOTf,'red')

title ('month4')

subplot(2,3,5)

plot(IC_TOTf,'red')

title ('month5')

subplot(2,3,6)

plot(IC_TOTf,'red')

title ('month6')

subplot(2,3,1)

plot(IC_TOTf,'red')

title ('month7')

subplot(2,3,2)

plot(IC_TOTf,'red')

title ('month8')

subplot(2,3,3)

plot(IC_TOTf,'red')
```

```
title ('month9')

subplot(2,3,4)

plot(IC_TOTf,'red')

title ('month10')

subplot(2,3,5)

plot(IC_TOTf,'red')

title ('month11')

subplot(2,3,6)

plot(IC_TOTf,'red')

title ('month12')

IC_TOTf;

 X_2=sum(IC_TOTf)

E_2=sum(p2)
```

Appendix C:

```
%% Location of Nablus, L=(32.13), LOD =(35.16)

clc

clear all

L = 32.13 ; %Latitude

LOD = 35.16 ; %Longitude

T_GMT = +3 ; % time diffrent with referance to GMT

step = 60 ; % time step

 Ni=[];

 IT_TOTf=[];

DSi=[];

p3=[];

 for N=365:-1:1

      Ni=[N;Ni];

DS = 23.45*(sind((360.*(N-81)./365))) ; %angle of declination

 DSi=[DS;DSi];

B = (360.*(N-81))/364 ;% equation of time
```

```
EOT = ((9.87.*sind(2*B)) - (7.53.*cosd(B))-(1.5.*sind(B))); %equa-
tion of time

LTM  = 15*T_GMT ;%local time meridian

if LOD >= 0

    TS_correction = (-4*(LTM - LOD))+ EOT ; % solar time correction

else

     TS_correction = (4*(LTM - LOD))+ EOT ; % solar time correction

end

Hsr_i = -tand(DS)*tand(L); % sun rise hour angle

Hsr = acosd(Hsr_i); %sun rise angle

STSR = abs(((Hsr/15)-12)*60); % sunrise solar time

STSS = abs(((Hsr/15)+12)*60); % sunset solar time

TSR = STSR + abs(TS_correction ); %actual time of sun rise

TSS = STSS + abs(TS_correction ); %actual time of sun set

sin_alpha_d = [];

Hsd=[];

for LMT=TSS : -step :TSR    %% for loop for the day time
```

```
        TS = LMT + TS_correction ;  %solar time

        HS = (15*(TS - (720)))./60 ; % hour angle degree

        sin_alpha_i = (sind(L).*sind(DS))+(cosd(L).*cosd(DS).*cosd(HS));
%altitude angle

        alpha = asind (sin_alpha_i);

        sin_alpha_d =[sin_alpha_i;sin_alpha_d];

        Hsd=[HS;Hsd];

   end

   sin_alpha_d;

   alpha_d=asind(sin_alpha_d);

   Hsd;

   for i=length(sin_alpha_d):-1:1

   alpha_d = asind(sin_alpha_d);

        %==============tracking\ %................solar radiation calcu-
lation for tracking surface

    A= 1160+(75*sind((360/365)*(N-275))); %solar energy flux

    K= 0.174+(0.035*sind((360/365)*(N-100))); %k is a factor

    C= 0.095+(0.04*sind((360/365)*(N-100))); %c is a factor
```

```
m =(1./sin_alpha_d(i)); %air mass

I_B =A.*exp(-K./m);%availabe beam radiation in the sky

IB_H =I_B.*( sin_alpha_d(i));%collected beam by collector in hori-
zantal surface

ID_H = C.*I_B ; %diffuse on horizantal surface

I_TOT =IB_H+ID_H ; %total radiatin

sin_PHI_Si =((sind(Hsd(i)).*cosd(DS))./cosd(alpha_d(i)));%azimuth
angleIB_H

PHI_S = asind(sin_PHI_Si);%azimuth angle

PHI_C = PHI_S;% azimuth angle of collector= azimuth angle of sun

beta1 = (90 - (alpha_d(i))) ;

cos_theta_t = ((cosd(alpha_d(i))*cosd(PHI_S-
PHI_C)*sind(beta1))+(sind(alpha_d(i) )*cosd(beta1)));%zineth angle

theta = acosd (cos_theta_t); %zineth angle

IB_T = I_B.*cos_theta_t ;%%collected beam by tracking system

ID_T = ID_H.* ((1+cosd(beta1))./2);%diffuse by tracking system

ROW = 0.2 ; % factor of reflection
```

```
 IR_T = ROW*(I_TOT).*((1-cosd(beta1))./2); %reflection by tracking
system

 IT_TOT =IB_T+ID_T+IR_T;

 IT_TOTf=[IT_TOT;IT_TOTf];

 p_T =  ((IT_TOT./1000).*(6*350));

 p3 =[ p_T ; p3];

 end

end

IT_TOTf;

 subplot(2,3,1)

plot (IT_TOTf, 'green')

title ('month1')

subplot(2,3,2)

plot (IT_TOTf, 'green')

title ('month2')

subplot(2,3,3)

plot (IT_TOTf, 'green')
```

```
title ('month3')

subplot(2,3,4)

plot (IT_TOTf, 'green')

title ('month4')

subplot(2,3,5)

plot (IT_TOTf, 'green')

title ('month5')

subplot(2,3,6)

plot (IT_TOTf, 'green')

title ('month6')

subplot(2,3,1)

plot (IT_TOTf, 'green')

title ('month7')

subplot(2,3,2)

plot (IT_TOTf, 'green')

title ('month8')

subplot(2,3,3)
```

```
plot (IT_TOTf, 'green')

title ('month9')

subplot(2,3,4)

plot (IT_TOTf, 'green')

title ('month10')

subplot(2,3,5)

plot (IT_TOTf, 'green')

title ('month11')

subplot(2,3,6)

plot (IT_TOTf, 'green')

title ('month12')

 x_3=sum(IT_TOTf)

 E_3=sum(p3)
```

Appendix D:

Item	Brand	origin	Qty	price
Solar Panels	sunket solar 430w Or Equivalent	china	5	2500
Inverter 2kw	Kaco Or Equivalent	Europe	1	1500
Solar Cables	DC Solar Cable	Europe	L.S	4.5 /m
AC Cable &Conduits ,Trunks	Ac cable	Turkey	L.S	8/M
DC CB	ABB or Phoenix	Europe	2	320
AC CB	ABB or Phoenix	Europe	2	360
Surge Arrester	ABB or Phoenix	Europe	2	200
MC4	MC4 connector	Europe	8	160
Junction Box	Water Proof local	local	2	250
Mounting Structure	Iron Galvanized local or Aluminum	local	L.S	280
Structure Accessories	Aluminum	china	L.S	50
earth leakage	ABB or Phoenix	Europe	1	160
Earthing Cable	6mm + 10mm	Europe	L.S	10/M
Wages work/ Transport				300/200
Profit of the company				1137
Price Seven thousand and four hundred and seventeen shekel			₪7417	
The exchange rate of the dollar against the shekel 1$ =3.4₪			2181$	

System Type: Stationary solar system.

* The price per kilowatt 1100$

Appendix F:

Item	Brand	origin	Qty	price
Solar Panels	sunket solar 430w Or Equivalent	china	5	2500
Inverter 2kw	Kaco Or Equivalent	Europe	1	1500
Solar Cables	DC Solar Cable	Europe	L.S	4.5 /m
AC Cable &Conduits ,Trunks	Ac cable	Turkey	L.S	8/M
DC CB	ABB or Phoenix	Europe	2	320
AC CB	ABB or Phoenix	Europe	2	360
Surge Arrester	ABB or Phoenix	Europe	2	200
MC4	MC4 connector	Europe	8	160
Junction Box	Water Proof local	local	2	250
Mounting Structure	Iron Galvanized local or Aluminum	local	L.S	280
Structure Accessories	Aluminum	china	L.S	50
earth leakage	ABB or Phoenix	Europe	1	160
Earthing Cable	6mm + 10mm	Europe	L.S	10/M
Wages work/ Transport				300/200
Profit of the company				1137
Solar system motor			1	7820
Price. Fifteen thousand two hundred and thirty-seven shekels			15237 ₪	
The exchange rate of the dollar against the shekel 1$ =3.4₪			**4481$**	

System Type: Tracked solar system.

* The price per kilowatt 2200$

Appendix E:

Data sheet for solar collector :

Control mode	Time+GPS
Tracking accuracy	0.1°- 2.0°(adjustable)
Gear motor power	24V/1.5A
Output torque	5000N·M
Tracking power consumption	＜0.125kwh per hour
Azimuth angle tracking range	100°
Elevation angle adjustment range	50°
Max. wind resistance in horizontal	＞40 m/s
Max. wind resistance in operation	＞24 m/s
Material	Hot-dipped galvanized＞65μm
Working temperature	-40℃ — +75℃
System Weight	150KG-250KG
Total power per set	1.5kW - 4.0kW

جامعة النجاح الوطنية

كلية الدراسات العليا

نمذجة إنتاجية الطاقة الشمسية لمُجمِّعات شمسية ثابتة ومائلة ومتتبِّعة في ظروف السماء الصافية: دراسة مقارنة

اعداد

اميرة إبراهيم مصطفى بهته

إشراف

د. تامر الخطيب

قدمت هذه الاطروحة استكمالا لمتطلبات الحصول على درجة الماجستير في هندسة الطاقة النظيفة وترشيد الاسنهلاك بكلية الدراسات العليا في جامعة النجاح الوطنية، نابلس– فلسطين

2020

نمذجة إنتاجية الطاقة الشمسية لمُجمِّعات شمسية ثابتة ومائلة ومتتبِّعة في ظروف السماء الصافية: دراسة مقارنة

اعداد

اميرة إبراهيم مصطفى بهته

إشراف

د. تامر الخطيب

الملخص

يعتبر إنتاج الطاقة الكهربائية القائمة على الإشعاع الشمسي من أهم الأولويات في عالم الطاقة النظيفة ، وأصبح التحدي الأكبر هو معرفة أي الأنظمة هي الأكثر إنتاجية للطاقة.

تم من خلال البحث الحالي تناول ثلاثة نماذج للأنظمة الكهروضوئية مصنفة حسب آلية عملها وهي كالآتي: النوع الأول هو المجمع الشمسي الأفقي ، والثاني هو المجمع الشمسي المائل ، والأخير هو المجمع الشمسي ثنائي المحور.

باستخدام برنامج الماتلاب ، وبناءً على ظروف السماء الصافية ، كان من المتوقع كمية الإشعاع الشمسي بواسطة كل من الأنظمة الثلاثة ، وكمية الطاقة الكهربائية التي يمكن إنتاجها في كل منها خلال ساعات النهار طوال فصل الصيف.

بعد ذلك ، أصبح من الواضح أن نظام المجمع الشمسي الذي يحتوي على تعقب ثنائي المحور هو أعلى إنتاجية للطاقة الكهربائية ، يليه النظام المائل ، وأخيراً النظام الأفقي. حيث ظهرت كمية الإنتاج الكهربائي لأنظمة تجميع الطاقة الشمسية الثلاثة على النحو التالي ، من أعلى إنتاجية إلى أدنى ، على التوالي 3709.71 كيلو واط ساعة ، 2476.30 كيلو واط ساعة ، 2366.75كيلو واط ساعة. من ناحية أخرى ، وهو الجانب الاقتصادي ، أثبت جهاز التعقب الشمسي أنه الأكثر اقتصادا ، فعلى الرغم من سعره المرتفع في بنائه ، إلا أنه كان أقل سعر للكيلوواط / ساعة بين الأنظمة الثلاثة ، حيث كان النظام الأفقي والمائل والمتتبع سجلت الأنظمة الأسعار التالية على

التوالي: 0.206 دولارًا لكل ساعة ، و 0.197 دولارًا لكل ساعة ، و 0.183 دولارًا لكل ساعة على التوالي.

في حين أن نموذج التتبع الشمسي ثنائي المحور هو الوحيد من بين النماذج المدروسة ، الذي يستهلك طاقة كهربائية أثناء عمله لأنه يحتوي على محرك للحركة من أجل تتبع الشمس ، فإن هذه الكمية المستهلكة كانت قليلة جدًا مقارنة بالطاقة المنتجة ، يكاد لا يذكر. لتجد أن هذا الأمر لم يؤثر على بقاء هذا النموذج في المقدمة من الناحيتين الانتاجية الكهربائية و الناحية الاقتصادية .